

LAPLACE AND DIRAC OPERATORS ON GRAPHS

BEATA CASIDAY, IVAN CONTRERAS, THOMAS MEYER, SABRINA MI, AND ETHAN SPINGARN

ABSTRACT. Discrete versions of the Laplace and Dirac operators haven been studied in the context of combinatorial models of statistical mechanics and quantum field theory. In this paper we introduce several variations of the Laplace and Dirac operators on graphs, and we investigate graph-theoretic versions of the Schrödinger and Dirac equation. We provide a combinatorial interpretation for solutions of the equations and we prove gluing identities for the Dirac operator on lattice graphs, as well as for graph Clifford algebras.

CONTENTS

1. Introduction	1
1.1. Acknowledgments	2
2. The graph Laplacian and the Schrödinger equation	3
2.1. Steady states	5
2.2. Average of quantum states	8
3. The graph Dirac operator and the Dirac equation	10
3.1. Matrix representations of graph Dirac operators	10
3.2. Visualization	12
3.3. Quadratic forms	14
3.4. Powers of \mathcal{D}_I	15
4. Dimer models and a gluing formula for Dirac operators	18
4.1. Graph gluing	18
4.2. The $2 \times n$ case	19
4.3. The $3 \times n$ case	20
4.4. The $4 \times n$ case	23
5. Spinors, Clifford algebras on graphs and gluing	27
5.1. Examples	28
5.2. Graph gluing and Clifford algebras	28
6. Future directions	32
Appendix: Algebraic computations for the gluing of lattice graphs	33
References	35

1. INTRODUCTION

The Laplace operator, or Laplacian, is a fundamental object of study in mathematics and physics. In particular, the evolution of quantum-mechanical systems is controlled by the Schrödinger equation, which relies on the properties of the Laplace operator. Discretized versions of the Laplacian have been implemented in order to study combinatorial models in quantum field theory [1, 9, 12]. Similarly, the Dirac operator (that can be understood as a *square root* of the Laplacian) is part of the mathematical formulation of spinors. One of the purposes of this paper is to study different versions of the Laplace and Dirac operators on finite graphs, and to analyze the (time dependent) Dirac equation on graphs, which gives a graph-theoretic interpretation of spinors. The notion of

spinor has its origins in particle physics: it first appeared around 1922 when Stern and Gerlach realized that electrons can be catalogued into two groups or streams (“up” or “down”), depending on a separation by a non-uniform magnetic field. It was later interpreted as a version of angular momentum, so the spin of a particle is naturally associated to the notion of rotation. Mathematically speaking, we can think of spinors as vectors in \mathbb{C}^2 . For instance, $\begin{bmatrix} 1 \\ 0 \end{bmatrix}$ can be seen as a spinor.

Spinors have natural linear transformations, which can be seen as rotations in \mathbb{R}^3 . More generally, it turns out that quaternions are useful to describe higher dimensional rotations, and therefore, spinors.

From the point of view of quantum mechanics, the dynamics of a quantum particle can be described in terms of the Schrödinger equation:

$$\partial_t(\psi) = \frac{i}{\hbar}\Delta(\psi), \quad (1)$$

where ψ is a state (a special type of function) and Δ is the Laplace operator:

$$\Delta = \nabla \cdot \nabla,$$

where ∇ denotes the gradient. Dirac provided a way to include particles with spin in the equation:

$$\not{\partial}(\psi) = \frac{mc}{i\hbar}\psi \quad (2)$$

where $\not{\partial}$ is called the Dirac operator, satisfying $\not{\partial}^2 = \Delta$.

A toy model of these equations is given in terms of the discrete Laplace and Dirac operators. The key advantage is that the evolution of states in this toy model depends only on the spectral properties of the graph. In particular, spectral graph theory analyzes the features of a graph in relationship with the behavior of the (eigenvalues/eigenvectors of) matrices associated with that graph.

Given the adjacency matrix A , and the degree matrix D , for a given graph Γ , the Laplacian $\Delta(\Gamma)$ of the graph is defined as the following matrix:

$$\Delta(\Gamma) = D(\Gamma) - A(\Gamma).$$

In Section 2 we introduce the even and odd graph Laplacian matrix, and the main results (Theorems 2.19 and 2.21) describe the steady states for the even and odd versions of the graph Schrödinger equations, in terms of the connected components and independent cycles of the graph.

In Section 3 we introduce various versions of the Dirac operator on graphs, including the *incidence Dirac operator* (Definition 3.3), inspired by the work of Knill [8]. The main result of this section (Theorem 3.14) is a graph-theoretic interpretation of the powers of the incidence Dirac operator, in terms of the number of certain walks on the graph.

A particular type of Dirac operators on graphs appears in the context of dimer models, following the work of Kenyon [5], Cimasoni and Reshetikhin [1]. It turns out that the Kasteleyn matrix, which produces the number of perfect matchings of lattice graphs, can be interpreted as a discrete Dirac operator. We prove (see Theorems 4.6, 4.7, 4.9, A.1) gluing formulae for different cases of graph gluing of lattice graphs. On the other hand, spinors have an algebraic representation via Clifford algebras. In Section 5 we follow the construction of Clifford algebras for graphs introduced by Khovanova in [7]. There it is described how to assign Clifford algebras to graphs. The main results (Theorems 5.5 and 5.6) provide an algebraic interpretation for the gluing of graphs in terms of their corresponding Clifford algebras.

1.1. Acknowledgments. This research project started during the 2021 SUMRY Program at Yale University, which was supported by NSF (DMS-2050398). I.C. thanks Pavel Mnev for useful discussions during the early stages of this project.

2. THE GRAPH LAPLACIAN AND THE SCHRÖDINGER EQUATION

The Laplacian describes the evolution of a quantum state over time for particles without spin, as governed by the Schrödinger equation. We study graph theoretic analogues of the Laplacian [10] and its interpretation in quantum mechanics [9]. We provide characterizations of the steady states of the graph Schrödinger equation and give a result on the average of quantum states.

We begin by defining quantum states on a graph. In the continuum, a quantum state is an assignment of a complex number to each point in space. We consider a graph theoretical model in which a graph quantum state is an assignment of a complex number to each vertex and each edge of a finite simple graph. This model can be considered as taking a "sampling" of points from the continuum and restricting our study to the evolution of this sample over time.

We next define several operators that are integral to our study of graph quantum mechanics.

Definition 2.1. Let $\Gamma = (V, E)$ be a finite simple graph. The *incidence matrix* of Γ , denoted I , is the $|V| \times |E|$ matrix whose (i, j) entry is defined by

$$[I]_{i,j} = \begin{cases} 1 & \text{edge } j \text{ ends at vertex } i \\ -1 & \text{edge } j \text{ starts at vertex } i \\ 0 & \text{otherwise.} \end{cases}$$

We use the incidence matrix to define the even and odd graph Laplacians. These operators act as discretized forms of the Laplace operator, and act on the vertices and edges of our graph respectively.

Definition 2.2. Let $\Gamma = (V, E)$ be a finite simple graph. A *vertex state* assigns a complex number to each vertex $v \in V$. An *edge state* assigns a complex number to each edge $e \in E$. A *vertex-edge state* assigns a complex number to each $v \in V$ and each $e \in E$.

Remark 1. When clear from context, we refer to these states as quantum states. In general, the even and odd Laplacian and Dirac operators act on vertex states and edge states respectively, and the incidence Dirac operator acts on vertex-edge states. We use the notation ψ to refer to a general quantum state, and use v and e to denote vertex and edge states respectively.

Definition 2.3. Let I be the incidence matrix of a finite simple graph Γ . The *Even Graph Laplacian* is defined as

$$\Delta_+ = II^t.$$

Equivalently, Δ_+ can be defined as

$$\Delta_+ = D - A,$$

where D and A are the degree and adjacency matrices of Γ respectively.

Definition 2.4. The *Odd Graph Laplacian* is defined as

$$\Delta_- = I^t I.$$

We now give a concrete example of the even and odd Laplacians on a small graph.

Example 2.5. Let Γ be the path graph with 3 vertices, and orientation given below.

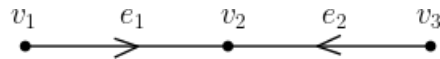


FIGURE 1. Oriented path graph P_3 .

Then the previously defined operators are given by:

$$I = \begin{bmatrix} -1 & 0 \\ 1 & 1 \\ 0 & -1 \end{bmatrix}$$

$$\Delta_+ = II^t = \begin{bmatrix} -1 & 0 \\ 1 & 1 \\ 0 & -1 \end{bmatrix} \begin{bmatrix} -1 & 1 & 0 \\ 0 & 1 & -1 \end{bmatrix} = \begin{bmatrix} 1 & -1 & 0 \\ -1 & 2 & -1 \\ 0 & -1 & 1 \end{bmatrix}$$

$$\Delta_- = I^t I = \begin{bmatrix} -1 & 1 & 0 \\ 0 & 1 & -1 \end{bmatrix} \begin{bmatrix} -1 & 0 \\ 1 & 1 \\ 0 & -1 \end{bmatrix} = \begin{bmatrix} 2 & 1 \\ 1 & 2 \end{bmatrix}.$$

Remark 2. By definition, we have $\Delta_+ = D - A$, so that the even Laplacian is independent of the orientation of Γ . In contrast, Δ_- does depend on orientation of the underlying graph, as shown in the following example.

Example 2.6. Let Γ_1 and Γ_2 be C_3 with the orientations given below:

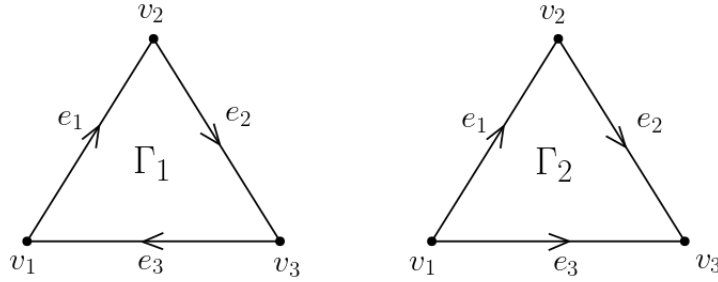


FIGURE 2. Two orientations of C_3 .

A routine calculation yields

$$\Delta_-(\Gamma_1) = \begin{bmatrix} 2 & -1 & -1 \\ -1 & 2 & -1 \\ -1 & -1 & 2 \end{bmatrix}$$

$$\Delta_-(\Gamma_2) = \begin{bmatrix} 2 & -1 & 1 \\ -1 & 2 & 1 \\ 1 & 1 & 2 \end{bmatrix}.$$

Remark 3. Eigenvalues of the odd Laplacian are independent of orientation. Indeed, for two graphs Γ_1 and Γ_2 of differing orientations, the odd Laplacians $\Delta_-(\Gamma_1)$ and $\Delta_-(\Gamma_2)$ are related by conjugation, hence have the same eigenvalues.

With these operators in hand, we introduce the discrete Schrödinger equation.

Definition 2.7. Let Γ be a finite simple graph with m vertices and n edges, and let $\psi : \mathbb{R} \rightarrow \mathbb{C}^m$ (\mathbb{C}^n) be a function assigning a complex number to each vertex (edge) of Γ . The *discrete Schrödinger equation* is defined as

$$\partial_t \psi = \frac{i}{\hbar} \Delta_{\pm} \psi.$$

Remark 4.

The following theorem [9] characterizes the solutions.

Theorem 2.8. *Solutions to the discrete Schrödinger equation are given by*

$$\psi(t) = e^{\frac{i}{\hbar} \Delta_{\pm} t} \psi(0).$$

From now on, we will write $\psi(0)$ as ψ_0 or simply ψ .

2.1. Steady states. We now proceed to characterize steady states of the even and odd graph Laplacians. These states are constant under the time evolution of the graph Schrödinger equation. From these steady states, we can extract graph-theoretic information on the connected components and independent cycles of our graph.

We show that steady states are in bijection with the kernels of the even and odd graph Laplacians, and identify these kernels accordingly.

Definition 2.9. A quantum state ψ_0 is a *steady state* if $e^{\frac{i}{\hbar}\Delta_{\pm}t}\psi_0 = \psi_0$ for all $t \geq 0$.

Theorem 2.10. Let A be an $n \times n$ matrix, $\psi_0 \in \mathbb{C}^n$ be a quantum state, $k \in \mathbb{C}$ be a nonzero complex constant, and t a complex variable. Then $e^{kAt}\psi_0 = \psi_0$ for all values of t if and only if $\psi_0 \in \ker(A)$.

Proof. (\Leftarrow) Suppose $\psi_0 \in \ker(A)$, so $A\psi_0 = 0$. Then

$$\begin{aligned} e^{kAt}\psi_0 &= \left(\sum_{n=0}^{\infty} \frac{(kAt)^n}{n!} \right) \psi_0 \\ &= \left(I + kAt + \frac{k^2 A^2 t^2}{2} + \frac{k^3 A^3 t^3}{3!} + \dots \right) \psi_0 \\ &= I\psi_0 + kAt\psi_0 + \frac{k^2 A^2 t^2}{2} \psi_0 + \frac{k^3 A^3 t^3}{3!} \psi_0 + \dots \\ &= I\psi_0 + kA\psi_0 t + \frac{k^2 A^2 \psi_0 t^2}{2} + \frac{k^3 A^3 \psi_0 t^3}{3!} + \dots \\ &= I\psi_0 + k(0)t + \frac{k^2 A(0)t^2}{2} + \frac{k^3 A^2(0)t^3}{3!} + \dots \\ &= I\psi_0 + 0 + 0 + 0 \dots = I\psi_0 = \psi_0. \end{aligned}$$

(\Rightarrow) Suppose $e^{kAt}\psi_0 = \psi_0$ for all values of t . Then $\frac{\partial}{\partial t} e^{kAt}\psi_0 = \frac{\partial}{\partial t} \psi_0$. The right-hand side of this equation equals 0 as ψ_0 is constant for all t . Now, considering the left hand side of this equation, we obtain:

$$\begin{aligned} \frac{\partial}{\partial t} e^{kAt}\psi_0 &= \frac{\partial}{\partial t} \left(\sum_{n=0}^{\infty} \frac{(kAt)^n}{n!} \right) \psi_0 \\ &= \frac{\partial}{\partial t} \left(I + kAt + \frac{k^2 A^2 t^2}{2} + \frac{k^3 A^3 t^3}{3!} + \dots \right) \psi_0 \\ &= \left(\frac{\partial}{\partial t} I + \frac{\partial}{\partial t} kAt + \frac{\partial}{\partial t} \frac{k^2 A^2}{2} t^2 + \frac{\partial}{\partial t} \frac{k^3 A^3}{3!} t^3 + \dots \right) \psi_0 \\ &= \left(0 + kA + k^2 A^2 t + \frac{k^3 A^3}{2} t^2 + \dots \right) \psi_0 \\ &= kA \left(I + kAt + \frac{k^2 A^2 t^2}{2} + \frac{k^3 A^3 t^3}{3!} + \dots \right) \psi_0 \\ &= kA e^{kAt} \psi_0. \end{aligned}$$

By assumption, $kA e^{kAt} \psi_0 = kA \psi_0$. This means $kA \psi_0 = 0$, so $\psi_0 \in \ker(A)$. ■

Since we have proven that steady states are in bijection with elements in the kernel of the graph Laplacians, it suffices to find the kernels of the even and odd graph Laplacians in order to characterize our steady states.

We now characterize the kernel of the even Laplacian. We begin with an intermediate lemma.

Lemma 2.11. Let Γ be a graph with connected components $\{1, 2, \dots, b_0\}$. A quantum state ψ is in $\ker \Delta_+$ if $\psi = 1$ on the vertices of the i th connected component, and 0 on all other vertices, for some $i \in \{1, \dots, b_0\}$.

We digress to provide a brief example, from which the general method of proof is clear.

Example 2.12. Let Γ be the oriented graph below, with two cycles and two connected components.

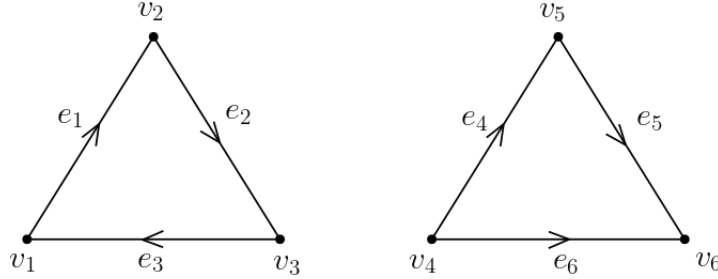


FIGURE 3. Oriented graph with two cycles and two connected components.

The even Laplacian of Γ is

$$\Delta_+ = \begin{bmatrix} 2 & -1 & -1 & 0 & 0 & 0 \\ -1 & 2 & -1 & 0 & 0 & 0 \\ -1 & -1 & 2 & 0 & 0 & 0 \\ 0 & 0 & 0 & 2 & -1 & -1 \\ 0 & 0 & 0 & -1 & 2 & -1 \\ 0 & 0 & 0 & -1 & -1 & 2 \end{bmatrix}.$$

Let $\psi = \begin{bmatrix} 1 \\ 1 \\ 1 \\ 0 \\ 0 \\ 0 \end{bmatrix}$ be the quantum state with entries 1 on the elements of the leftmost connected component of the graph, and 0 on all other vertices. We immediately see that

$$\Delta_+ \psi = \begin{bmatrix} 2 & -1 & -1 & 0 & 0 & 0 \\ -1 & 2 & -1 & 0 & 0 & 0 \\ -1 & -1 & 2 & 0 & 0 & 0 \\ 0 & 0 & 0 & 2 & -1 & -1 \\ 0 & 0 & 0 & -1 & 2 & -1 \\ 0 & 0 & 0 & -1 & -1 & 2 \end{bmatrix} \begin{bmatrix} 1 \\ 1 \\ 1 \\ 0 \\ 0 \\ 0 \end{bmatrix} = 0,$$

so that ψ is in the kernel of Δ_+ as was claimed in our lemma.

We now proceed to a formal proof of this lemma.

Proof. Let Γ be a graph with n vertices. Let v_1, v_2, \dots, v_k be the vertices of a connected component of Γ .

Let

$$\Delta_+ = \begin{bmatrix} \Delta_{1,1} & \dots & \Delta_{1,n} \\ \vdots & \ddots & \vdots \\ \Delta_{n,1} & \dots & \Delta_{n,n} \end{bmatrix}$$

and let

$$\psi = \begin{bmatrix} 1 \\ \vdots \\ 1 \\ 0 \\ \vdots \\ 0 \end{bmatrix}$$

be the column vector with values $[\psi]_{i,1} = \begin{cases} 1 & 1 \leq i \leq k \\ 0 & k < i \leq n \end{cases}$.

Multiplying by the even Laplacian, we observe that

$$\Delta_+ \psi = \begin{bmatrix} \Delta_{1,1} \cdot 1 + \cdots + \Delta_{1,k} \cdot 1 + \Delta_{1,k+1} \cdot 0 + \cdots + \Delta_{1,n} \cdot 0 \\ \vdots \\ \Delta_{k,1} \cdot 1 + \cdots + \Delta_{k,k} \cdot 1 + \Delta_{k,k+1} \cdot 0 + \cdots + \Delta_{k,n} \cdot 0 \\ \Delta_{k+1,1} \cdot 1 + \cdots + \Delta_{k+1,k} \cdot 1 + \Delta_{k+1,k+1} \cdot 0 + \cdots + \Delta_{k+1,n} \cdot 0 \\ \vdots \\ \Delta_{n,1} \cdot 1 + \cdots + \Delta_{n,k} \cdot 1 + \Delta_{n,k+1} \cdot 0 + \cdots + \Delta_{n,n} \cdot 0 \end{bmatrix} = \begin{bmatrix} \Delta_{1,1} + \cdots + \Delta_{1,k} \\ \vdots \\ \Delta_{k,1} + \cdots + \Delta_{k,k} \\ \Delta_{k+1,1} \cdots + \Delta_{k+1,k} \\ \vdots \\ \Delta_{n,1} + \cdots + \Delta_{n,k} \end{bmatrix}.$$

Recall that $\Delta_+ = D - A$, where D and A denote the degree and adjacency matrices of Γ respectively. Thus, for all $\Delta_{i,j}$ with $i > j$ and $j \in \{1, 2, \dots, k\}$, we have $\Delta_{i,j} = 0$, as vertices i and j are in different connected components of Γ . Thus, we have

$$\Delta_+ \psi = \begin{bmatrix} \Delta_{1,1} + \cdots + \Delta_{1,k} \\ \vdots \\ \Delta_{k,1} + \cdots + \Delta_{k,k} \\ \Delta_{k+1,1} \cdots + \Delta_{k+1,k} \\ \vdots \\ \Delta_{n,1} + \cdots + \Delta_{n,k} \end{bmatrix} = \begin{bmatrix} \Delta_{1,1} + \cdots + \Delta_{1,k} \\ \vdots \\ \Delta_{k,1} + \cdots + \Delta_{k,k} \\ 0 \\ \vdots \\ 0 \end{bmatrix}.$$

Note that both $D(v_i)$ and $\sum_{j=1}^k A_{i,j}$ count the number of edges incident to the vertex v_i , hence are equal. Thus, we obtain our desired result, as by definition we have $\Delta_{i,1} + \cdots + \Delta_{i,k} = D(v_i) - \sum_{j=1}^k A_{i,j} = 0$, so that $\Delta_+ \psi = 0$ as desired. \blacksquare

Lemma 2.13. A quantum state is in the kernel of the even Laplacian if and only if it is constant on each of the connected components of the graph.

Proof. From [3], we know that $\dim(\ker \Delta_+) = b_0$. Label our connected components $\{1, 2, \dots, b_0\}$. Let ψ_i be the vertex state with the value 1 on the vertices of the i th connected component, and 0 on all other vertices. By the above lemma, each of these ψ_i is in the kernel of Δ_+ . Furthermore, each ψ_i is linearly independent, and we have one ψ_i for each connected component, so these ψ_i must span $\ker \Delta_+$ as desired. \blacksquare

Corollary 2.14. A vertex state ψ is steady if and only if ψ is constant on each of the graph's connected components.

Proof. Combining results 2.10 and 2.13, we see that a vertex state is steady if and only if it is in the kernel of the even Laplacian if and only if it is constant on a graph's connected components. \blacksquare

Corollary 2.15. The vector space of steady vertex states is isomorphic to \mathbb{C}^{b_0} .

2.2. Average of quantum states. We now proceed to characterize quantum states (both vertex and edge states) which have a constant average under the Schrödinger equation.

Definition 2.16. Let $\psi = \begin{bmatrix} z_1 \\ z_2 \\ \vdots \\ z_n \end{bmatrix}$ be a vertex state of a graph. We define the *average of ψ* to be

$$\mu(\psi) = \frac{z_1 + z_2 + \cdots + z_n}{n}.$$

Definition 2.17. Let Δ_{\pm} denote the even and odd graph Laplacians. The *partition function of Δ_{\pm}* is defined to be

$$Z(t) = e^{\frac{i}{\hbar}\Delta_{\pm}t}.$$

Remark 5. The even Laplacian is a real symmetric matrix so it is Hermitian.

Lemma 2.18. The partition function of a Hermitian matrix is unitary. In particular, the partition function of the even Laplacian is unitary.

Proof. Let A be a Hermitian matrix; that is, $A = \overline{A}^T$. We want to show $e^{iA} = I + iA + \frac{(iA)^2}{2} + \frac{(iA)^3}{3!} + \dots$ is unitary; that is, $\overline{e^{iA}}^T = e^{-iA}$. There are a few linear algebra facts that will be useful in this proof:

- (1) $\overline{A + B}^T = \overline{A}^T + \overline{B}^T$
- (2) $\overline{(A^n)}^T = (\overline{A}^T)^n$
- (3) $\overline{iA} = \overline{i} \overline{A} = -i\overline{A}$.

The proof consists of a string of equalities:

$$\begin{aligned} \overline{e^{iA}}^T &= \overline{I + iA + \frac{(iA)^2}{2} + \frac{(iA)^3}{3!} + \cdots}^T \\ &= I + \overline{iA}^T + \frac{\overline{(iA)^2}^T}{2} + \frac{\overline{(iA)^3}^T}{3!} + \cdots \\ &= I + \overline{iA}^T + \frac{(\overline{iA}^T)^2}{2} + \frac{(\overline{iA}^T)^3}{3!} + \cdots \\ &= I + -i\overline{A}^T + \frac{(-i\overline{A}^T)^2}{2} + \frac{(-i\overline{A}^T)^3}{3!} + \cdots \\ &= I + -iA + \frac{(-iA)^2}{2} + \frac{(-iA)^3}{3!} + \cdots \\ &= e^{-iA}. \end{aligned}$$

■

Theorem 2.19. For a vertex state ψ_0 , the average $\mu(\psi_0) = \mu(\psi_t)$ for all $t \geq 0$.

Proof. Let $\psi_0 = \begin{bmatrix} z_1 \\ z_2 \\ \vdots \\ z_n \end{bmatrix}$ be a vertex state on a graph. The average of ψ_0 can be given by the inner

product $\langle v, \psi_0 \rangle$, where $v = \begin{bmatrix} \frac{1}{n} \\ \frac{1}{n} \\ \vdots \\ \frac{1}{n} \end{bmatrix}$. The partition function $Z(t) = e^{\frac{i}{\hbar}\Delta_{\pm}t}$ of the even Laplacian is

unitary, hence preserves inner product. From this, we have

$$\mu(\psi_0) = \langle v, \psi_0 \rangle = \langle Z(t)v, Z(t)\psi_0 \rangle = \langle v, \psi_t \rangle = \mu(\psi_t),$$

where the equality $Z(t)v = v$ follows as v is a steady state (constant on all vertices), and $Z(t)\psi_0 = \psi_t$ simply denotes a solution to the Schrödinger equation over time. Thus the average is constant as desired. \blacksquare

Having characterized the steady states of the even graph Schrödinger equation, we now turn our attention to the odd graph Schrödinger equation.

Definition 2.20. Recall that the first Betti number b_1 is equivalent to the dimension of the cycle space of a graph. Let c_1, c_2, \dots, c_{b_1} be the independent cycles of a graph Γ . To each independent cycle c_i , we define the *independent cycle edge state* α_i to be the edge state with value 1 on all edges with clockwise orientation on c_i , -1 on all edges with counterclockwise orientation on c_i , and 0 on all edges not in c_i .

Theorem 2.21. *An edge state ψ is steady for the odd Schrödinger if and only if ψ represents a linear combination of independent cycle edge states.*

Note that this theorem is not independent of orientation; that is, two orientations of the same graph may admit two different spaces of steady states of the odd Laplacian.

Let us consider C_3 with the same orientations as in Example 2.6. The theorem above tells us that the leftmost graph has steady states $\ker(\Delta_-) = \text{span} \left\{ \begin{bmatrix} 1 \\ 1 \\ 1 \end{bmatrix} \right\}$, while the rightmost graph has

steady states $\ker(\Delta_-) = \text{span} \left\{ \begin{bmatrix} 1 \\ 1 \\ -1 \end{bmatrix} \right\}$. With this example in hand, we now prove the theorem

in general.

Proof. By 2.10, it suffices to show that the kernel of Δ_- is spanned by linear combinations of independent cycles. To this end, we show that every vector representing an independent cycle is in the kernel of the incidence matrix.

We first consider the action of the incidence matrix on a single edge e_k ; that is, on the edge state with value 1 on the edge e_k , and value 0 on all remaining edges. By definition, we have

$$[I]_{i,j} = \begin{cases} -1 & \text{edge } e_j \text{ begins at vertex } v_i \\ 1 & \text{edge } e_j \text{ ends at vertex } v_i \\ 0 & \text{otherwise.} \end{cases}$$

Let $v_{e_k,i}$ and $v_{e_k,f}$ denote the initial and final vertices of e_k respectively. By the above definition, using a slight abuse of notation, we see that $Ie_k = v_{e_k,f} - v_{e_k,i}$ (where here, e_k , $v_{e_k,i}$, and $v_{e_k,i}$ represent the edge and vertex states with value 1 on e_k , $v_{e_k,i}$, and $v_{e_k,i}$ respectively and 0 on all other edges and vertices).

We now consider the action of I on an independent cycle edge state. Let α_i be an independent cycle edge state. We may decompose α_i into a sum of its individual edges $\alpha_i = e_{i,1} + e_{i,1} + \dots + e_{i,k_i}$. Without loss of generality, we may assume the final vertex of each edge $e_{i,j}$ is the initial vertex of the edge $e_{i,j+1}$ and the final vertex of e_{i,k_i} is the initial vertex of $e_{i,1}$. By linearity, we obtain $I\alpha_i = Ie_{i,1} + Ie_{i,2} + \dots + Ie_{i,k_i}$. Combining this with our previous consideration of the action of I on individual edges, we know

$$Ie_{i,1} + Ie_{i,2} + \dots + Ie_{i,k_i} = (v_{e_{i,1},f} - v_{e_{i,1},i}) + (v_{e_{i,2},f} - v_{e_{i,2},i}) + \dots + (v_{e_{i,k_i},f} - v_{e_{i,k_i},i}).$$

Since we have chosen our independent cycle edge states to have value 1 on clockwise oriented edges and -1 on counterclockwise oriented edges, and our edges are assumed to be consecutive, we see that

$$(v_{e_1,f} - v_{e_1,i}) + (v_{e_2,f} - v_{e_2,i}) + \cdots + (v_{e_{k_i},f} - v_{e_{k_i},i}) = (v_{e_1,f} - v_{e_{k_i},f}) + (v_{e_2,f} - v_{e_1,f}) + \cdots + (v_{e_{k_i},f} - v_{e_{k_i-1},f}).$$

This sum telescopes to the zero vector as desired.

From this, we see that all independent cycle edge states are in $\ker(\Delta_-)$; indeed, for an independent cycle edge state α , by the above we have

$$\Delta_- \alpha = I^t I \alpha = 0,$$

so that $\alpha \in \ker(\Delta_-)$ as desired.

Lastly, recall that $\dim \ker(\Delta_-) = b_1$. Each independent cycle edge state is linearly independent, and moreover, we have precisely b_1 of these states, so that the kernel of Δ_- is equal to the span of independent cycle edge states. Thus by Theorem 2.10, we see that a state is steady if and only if it is a linear combination of independent cycle edge states as desired. \blacksquare

3. THE GRAPH DIRAC OPERATOR AND THE DIRAC EQUATION

3.1. Matrix representations of graph Dirac operators. We now proceed to consider the graph Dirac operators. These operators can be viewed as formal square roots of the graph Laplacians. Note that both the even and odd Laplacian are real symmetric matrices, hence are diagonalizable.

Let $Q_+ D_+ Q_+^{-1}$ and Q_-, D_-, Q_-^{-1} be the diagonalizations of the even and odd Laplacians respectively. Let $\sqrt{D_\pm}$ be the matrix given by taking the square root of each diagonal entry. The graph Dirac operators are defined as follows.

Definition 3.1. The *Even Dirac operator* is defined as $\mathcal{D}_+ = Q_+ \sqrt{D_+} Q_+^{-1}$.

Definition 3.2. The *Odd Dirac operator* is defined as $\mathcal{D}_- = Q_- \sqrt{D_-} Q_-^{-1}$.

To see that the above operators serve as formal square roots of the even and odd Laplacians, note that we have

$$(\mathcal{D}_\pm)^2 = Q_\pm \sqrt{D_\pm} Q_\pm^{-1} Q_\pm \sqrt{D_\pm} Q_\pm^{-1} = \Delta_\pm,$$

as desired.

Definition 3.3. The *Incidence Dirac operator* is defined as $\mathcal{D}_I = \begin{pmatrix} 0 & I \\ I^t & 0 \end{pmatrix}$.

The incidence Dirac operator also serves as a formal square root of the Laplace operators, as we have

$$(\mathcal{D}_I)^2 = \begin{pmatrix} \Delta_+ & 0 \\ 0 & \Delta_- \end{pmatrix}.$$

In this section, we study the linear algebraic properties of the graph Dirac operators. In particular, we prove $\ker \mathcal{D}_\pm = \ker \Delta_\pm$ and $\ker \mathcal{D}_I = \ker \mathcal{D}_+ \oplus \ker \mathcal{D}_-$. Additionally, we prove a relationship between the nonzero eigenvalues of \mathcal{D}_I and the nonzero eigenvalues of Δ_\pm .

Proposition 3.4. $\ker I^t = \ker \Delta^+$ and $\ker I = \ker \Delta^-$.

Proof. We prove the first equality; the second follows analogously. We first show $\ker I^t \subseteq \ker \Delta_+$. Indeed, suppose $v \in \ker I^t$. Then $\Delta_+ v = I(I^t v) = 0$, so $v \in \ker \Delta_+$. Conversely, suppose $v \in \ker \Delta_+$. Then $\Delta_+ v = I I^t v = 0$, so that $v^t (I I^t v) = (I^t v)^t (I v) = \|I^t v\|^2 = 0$, so that $I^t v = 0$ as desired. \blacksquare

Proposition 3.5. \mathcal{D}_+ and \mathcal{D}_- are non-negative definite matrices, $\ker \mathcal{D}_+ = \ker \Delta_+$, and $\ker \mathcal{D}_- = \ker \Delta_-$.

Proof. We first claim that \mathcal{D}_+ is non-negative definite. Let QDQ^{-1} be the diagonalization of Δ_+ . Since Δ_+ is non-negative definite, all entries in the matrix D will be non-negative, so that all entries in the diagonal matrix \sqrt{D} of $\mathcal{D}_+ = Q\sqrt{D}Q^{-1}$ will be non-negative. Thus, the eigenvalues of \mathcal{D}_+ are non-negative, so \mathcal{D}_+ is non-negative definite as desired.

We next claim that $\ker \mathcal{D}_+ = \ker \Delta_+$. To this end, we show that $\ker \mathcal{D}_+ \subseteq \ker \Delta_+$, and $\dim \ker \mathcal{D}_+ = \dim \ker \Delta_+$.

To see the first of these claims, let $v \in \ker \mathcal{D}_+$. By definition $\mathcal{D}_+v = 0$, so that $\Delta_+v = \mathcal{D}_+(\mathcal{D}_+v) = 0$. Thus we have $v \in \ker \Delta_+$ as desired.

We now demonstrate the second claim. Let $\lambda_1, \lambda_2, \dots, \lambda_n$ be the eigenvalues of Δ_+ . By definition, we see the eigenvalues of \mathcal{D}_+ are $\sqrt{\lambda_1}, \sqrt{\lambda_2}, \dots, \sqrt{\lambda_n}$.

Recall that $\dim \ker \Delta_+$ is precisely the geometric multiplicity of the eigenvalue 0. From the above, we see that the algebraic multiplicities of 0 for Δ_+ and \mathcal{D}_+ are equal. Each of these matrices are diagonalizable, hence the geometric multiplicities of 0 for Δ_+ and \mathcal{D}_+ are equal, so that $\dim \ker \Delta_+ = \dim \ker \mathcal{D}_+$ as desired.

Similarly, \mathcal{D}_- is a non-negative definite matrix and $\ker \mathcal{D}_- = \ker \Delta_-$. ■

Remark 6. We know that $\ker \Delta_+ \cong \mathbb{C}^{b_0}$ and $\ker \Delta_- \cong \mathbb{C}^{b_1}$, so by the above we have $\ker \mathcal{D}_+ \cong \mathbb{C}^{b_0}$ and $\ker \mathcal{D}_- \cong \mathbb{C}^{b_1}$.

Proposition 3.6. $\ker \mathcal{D}_I = \ker \Delta^+ \oplus \ker \Delta^-$.

Proof. We first prove that $\ker \mathcal{D}_I = \ker I^t \oplus \ker I$. Let $v = \begin{bmatrix} x \\ y \end{bmatrix}$ where $x \in \mathbb{C}^{|V|}$ and $y \in \mathbb{C}^{|E|}$. By definition, we see

$$v \in \ker \mathcal{D}_I \iff \begin{bmatrix} 0 & I \\ I^t & 0 \end{bmatrix} \begin{bmatrix} x \\ y \end{bmatrix} = 0 \iff \begin{bmatrix} Iy \\ I^tx \end{bmatrix} = \begin{bmatrix} 0 \\ 0 \end{bmatrix}.$$

Thus we see $v = \begin{bmatrix} x \\ y \end{bmatrix} \in \ker \mathcal{D}_I \iff x \in \ker I^t$ and $y \in \ker I$ so that by proposition 3.4 we have

$$\ker \mathcal{D}_I = \ker I^t \oplus \ker I = \ker \Delta^+ \oplus \ker \Delta^-.$$
■

Proposition 3.7. *The eigenvalues of \mathcal{D}_I are independent of orientation.*

Proof. Let Γ and Γ' be two orientations of the same graph. Let v be a vertex state on this graph,

and let $e = \begin{pmatrix} e_1 \\ e_2 \\ \vdots \\ e_n \end{pmatrix}$ be an edge state on this graph. Without loss of generality, assume Γ and Γ'

differ on edges e_1, \dots, e_k . Suppose $\mathcal{D}_I(\Gamma) \begin{pmatrix} v \\ e \end{pmatrix} = \lambda \begin{pmatrix} v \\ e \end{pmatrix}$, so that λ is an eigenvalue of Γ . Then $I(\Gamma)e = \lambda v$ and $I^t(\Gamma)v = \lambda e$. By definition of the incidence matrix, for each $i \leq k$, we have

$$\text{col}_i(I(\Gamma')) = -\text{col}_i(I(\Gamma)), \text{ so that } I(\Gamma') \begin{pmatrix} -e_1 \\ \vdots \\ -e_k \\ e_{k+1} \\ \vdots \\ e_n \end{pmatrix} = I(\Gamma)e = \lambda v.$$

Because $I^t(\Gamma)v = \lambda e$, we know from the relationship between their columns that $I^t(\Gamma')v =$

$$\lambda \begin{pmatrix} -e_1 \\ \vdots \\ -e_k \\ e_{k+1} \\ \vdots \\ e_n \end{pmatrix}. \text{ Thus, } \mathcal{D}_I(\Gamma') \begin{pmatrix} v \\ -e_1 \\ \vdots \\ -e_k \\ e_{k+1} \\ \vdots \\ e_n \end{pmatrix} = \lambda \begin{pmatrix} v \\ -e_1 \\ \vdots \\ -e_k \\ e_{k+1} \\ \vdots \\ e_n \end{pmatrix}, \text{ so } \lambda \text{ is an eigenvalue for } \mathcal{D}_I(\Gamma'). \quad \blacksquare$$

Corollary 3.8. *The non-zero eigenvalues of \mathcal{D}_I are $-\sqrt{\lambda_1}, \sqrt{\lambda_1}, -\sqrt{\lambda_2}, \sqrt{\lambda_2}, \dots, -\sqrt{\lambda_n}, \sqrt{\lambda_n}$, where $\lambda_1, \dots, \lambda_n$ are the non-zero eigenvalues of Δ_{\pm} .*

Proof. Let $\lambda_1, \dots, \lambda_n$ be the nonzero eigenvalues of Δ_{\pm} . Because $\mathcal{D}_I^2 = \begin{bmatrix} \Delta_+ & O \\ O & \Delta_- \end{bmatrix}$, we have $P_{\mathcal{D}_I^2}(t) = P_{\Delta_+}(t) \cdot P_{\Delta_-}(t)$, where $P_A(t)$ denotes the characteristic polynomial of a matrix A .

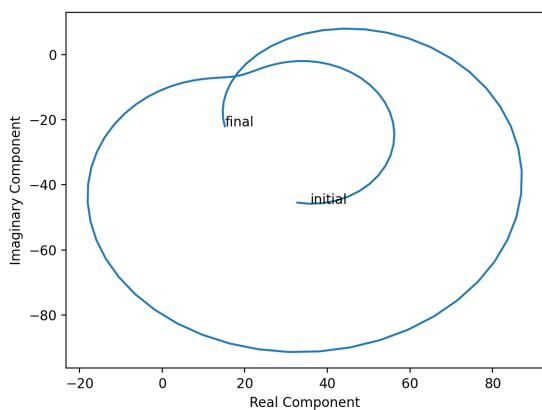
Because $\mathcal{D}_I^2 = \begin{bmatrix} \Delta_+ & O \\ O & \Delta_- \end{bmatrix}$, we have $P_{\mathcal{D}_I^2}(t) = P_{\Delta_+}(t) \cdot P_{\Delta_-}(t)$, where $P_A(t)$ denotes the characteristic polynomial of a matrix A . We know that Δ_+ and Δ_- have the same eigenvalues with the same multiplicity, so the non-zero eigenvalues of \mathcal{D}_I^2 are $\lambda_1, \lambda_1, \lambda_2, \lambda_2, \dots, \lambda_n, \lambda_n$. Then the non-zero eigenvalues of \mathcal{D}_I are $\pm\sqrt{\lambda_1}, \pm\sqrt{\lambda_1}, \dots, \pm\sqrt{\lambda_n}, \pm\sqrt{\lambda_n}$. If a is an eigenvalue of \mathcal{D}_I , then $-a$ is an eigenvalue of $-\mathcal{D}_I$. Because this is equivalent to the Incidence Dirac for the same graph with the opposite orientations, Proposition 3.7 tells us that $-a$ must also be an eigenvalue for \mathcal{D}_I . This means that for each pair of $\pm\sqrt{\lambda_i}$ eigenvalues, if one is positive the other must be negative, and vice-versa. \blacksquare

3.2. Visualization. We implemented a program in Python which computes solutions to the different versions of the Dirac equation over time, given a random graph and initial random quantum state (vertex state for even Dirac operator, edge state for odd Dirac operator, vertex and edge state for incidence Dirac operator).

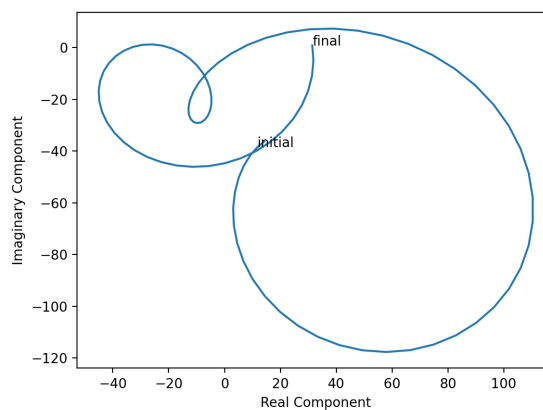
We plotted average position and average angle of these solutions over time, where average position is given as the average of real components and the average of imaginary components, and average angle is given as the angle formed by the coordinates of the average position in the complex plane.

Figure 4 is a typical plot of average position over time for solutions to the Dirac equation for the even, odd, and incidence Dirac operators, for a random graph with 10 vertices.

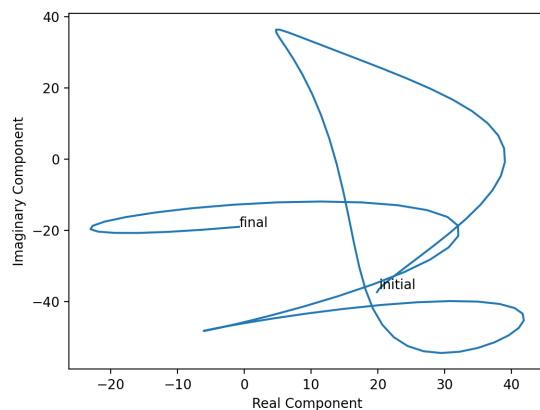
The geometric features of these plots can yield information to the behavior of the quantum system over time. As a brief example, consider a quantum state which is constant on each connected component of a graph. By corollary 2.14, we know that such a quantum state is steady over time. Figure 5 plots the average angle and position over time of a quantum state in the kernel of a graph. The nonconstant behavior of the graph is due to rounding error in Python.



(A) Even Dirac operator.

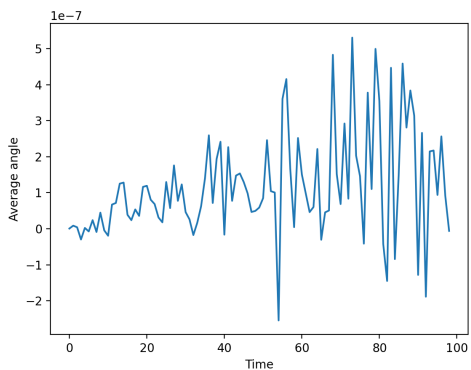


(B) Odd Dirac operator.

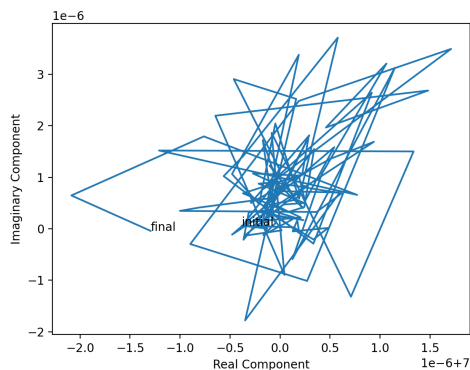


(C) Incidence Dirac operator.

FIGURE 4. Plots of average position over time for a random quantum state.



(A) average angle over time.



(B) average position in complex plane.

FIGURE 5. Plots of a vertex state in the kernel of the even Dirac operator.

3.3. Quadratic forms. We can encode information on the eigenvalues of the graph operators via their quadratic forms, as their signatures provide invariants of the graph, which determine the behavior of the solutions of the graph Schrödinger and Dirac equations.

Definition 3.9. For a symmetric matrix M , its associated quadratic form is defined as $q_M(v) = v^t M v$

Using this definition we find graph theoretical expressions for the quadratic forms of our graph operators. For instance, it is well known [10] that the quadratic form of Δ_+ is

$$q_{\Delta_+}(v) = \sum_{e_{i,j} \in E(\Gamma)} (v_j - v_i)^2. \quad (3)$$

We find similar expressions for the quadratic forms of other operators. Where the even Laplacian sums a function on the vertices over the edges, the odd Laplacian sums a similar function on the edges over the vertices.

Proposition 3.10. *The quadratic form of the odd Laplacian is*

$$q_{\Delta_-}(e) = \sum_{v_i \in V(\Gamma)} \left(\sum_{e_{i,j} \in E(\Gamma)} k_{i,j} \cdot e_{i,j} \right)^2,$$

$$\text{where } k_{i,j} = \begin{cases} -1 & e_{i,j} \text{ leaves } v_i \\ 1 & e_{i,j} \text{ enters } v_i \end{cases}.$$

Proof. From the definition of the odd Laplacian, we have that

$$\Delta_-(i,j) = \begin{cases} 2 & i = j \\ 0 & i \neq j, e_i \text{ not incident to } e_j \\ 1 & i \neq j, e_i \text{ incident to } e_j, \text{ both start or end at } v_s \\ -1 & i \neq j, e_i \text{ incident to } e_j, \text{ one starts and the other ends at } v_s. \end{cases}$$

For each $v_s \in V(\Gamma)$, there are $\frac{D(v_s)(D(v_s)-1)}{2}$ terms of the form $(-1)^k 2e_{i,s} \cdot e_{j,s}$, where $k = 0$ when e_i and e_j both start or end at v_s and $k = 1$ when one starts and the other ends at v_s . The diagonal adds the term $2e_{i,j}^2$ to the quadratic form. Each edge is incident to exactly two vertices, thus we assign a squared term to each of these vertices. Thus for each v_s , we have

$$\sum_{e_{i,s} \in E(\Gamma)} \left(e_{i,s}^2 + \sum_{e_{j,s} \neq e_{i,s} \in E(\Gamma)} (-1)^k 2e_{i,s} \cdot e_{j,s} \right)$$

in this quadratic form. Because each $e_{i,s}$ which appears in the second sum will appear in our first, this sum is equal to

$$\left(\sum_{e_{i,s} \in E(\Gamma)} k_{i,s} e_{i,s} \right)^2,$$

where $k = -1$ if an edge starts at v_s and $k = 1$ if it ends at v_s .

Adding these terms for each vertex finishes the proof. ■

Proposition 3.11. *The quadratic form of the incidence Dirac operator \mathcal{D}_I is*

$$q_{\mathcal{D}_I} \begin{pmatrix} v \\ e \end{pmatrix} = 2 \sum_{e_{i,j} \in E(\Gamma)} e_{i,j} \cdot (v_j - v_i).$$

Proof. Because $(v^t \ e^t) \mathcal{D}_I \begin{pmatrix} v \\ e \end{pmatrix} = v^t I e + e^t I^t v$, and these 1×1 matrices are transposes of one another, they are equal, giving $(v^t \ e^t) \mathcal{D}_I \begin{pmatrix} v \\ e \end{pmatrix} = 2e^t I^t v$. Each row of I^t represents some $e_{i,j}$, and returns $v_j - v_i$ (where $e_{i,j}$ goes from v_j to v_i), so when we multiply this out, we get $\sum_{e_{i,j} \in E(\Gamma)} e_{i,j} \cdot (v_j - v_i)$. ■

Because the roots of the quadratic form of a non-negative definite matrix are exactly the vectors in the kernel of the matrix, the set of roots of $q_{\Delta_{\pm}}$ (denoted by $\text{root}(q_{\Delta_{\pm}})$) provides important graph-theoretical information. Specifically, $q_{\Delta_+}(v) = 0$ if and only if v is constant on connected components, and $q_{\Delta_-}(e) = 0$ if and only if e represents a cycle on the graph. Interestingly, there is not a similar equality for \mathcal{D}_I , as stated in the following proposition.

Proposition 3.12.

$$\text{root}(q_{\mathcal{D}_I}) \supseteq \ker(\Delta_+) \oplus \mathbb{C}^{|E|} \cup \mathbb{C}^{|V|} \oplus \ker(\Delta_-).$$

Proof. If $v \in \ker(\Delta_+)$, then we know v is constant on connected components, so $v_j - v_i = 0$ for each $e_{i,j} \in E(\Gamma)$. Then for any e , we will have that $q_{\mathcal{D}_I}(v \oplus e) = 0$.

For $e \in \ker(\Delta_-)$, any non-zero terms of e must be a part of a cycle, so by definition of $q_{\mathcal{D}_I}$, each v_i will be added and subtracted exactly once on the cycle (if an edge goes in the opposite direction to an incident edge, the edge term must have the opposite sign to be in the kernel). From the properties of $\ker(\Delta_-)$, the terms by which these vertex terms are multiplied will be equal, so $v \oplus e$ is a root of our quadratic for any v . ■

Because the eigenvalues of the Incidence Dirac operator come in pairs of positive and negative values, it is not non-negative definite, so the root of the quadratic form doesn't match with the kernel of the matrix as it did for the Laplace operators. For this reason, it is not clear what the entire root of $q_{\mathcal{D}_I}$ would look like for most graphs.

An example of a graph where we can see the entire root of $q_{\mathcal{D}_I}$ is P_2 , for which we have

$$\mathcal{D}_I = \begin{pmatrix} 0 & 0 & -1 \\ 0 & 0 & 1 \\ -1 & 1 & 0 \end{pmatrix}.$$

Here, if $v \oplus e \in \text{root}(q_{\mathcal{D}_I})$, we must have that either $e = 0$ or $v_1 = v_2$, so in this case $\text{root}(q_{\mathcal{D}_I}) = \ker(\Delta_+) \oplus \mathbb{C}^{|E|} \cup \mathbb{C}^{|V|} \oplus \ker(\Delta_-)$

By contrast, cycle graphs will have many roots which are not a part of this union. For example,

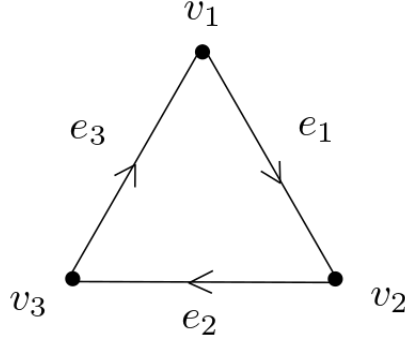
the vector $\begin{pmatrix} 1 \\ 2 \\ 2 \\ 2 \\ 1 \\ 2 \end{pmatrix}$ is a root for $q_{\mathcal{D}_I}$ for the oriented graph in Figure 6.

3.4. Powers of \mathcal{D}_I . An interesting property of the Laplace operators is the fact that the entries of the powers of these matrices encode combinatorial information about superwalks on the graph, as explained by [13].

A *vertex superwalk* of length 1 starting at v_i can

- (1) go through an incident edge to one of it's neighbors, in which case $\text{sgn}(\gamma) = -1$, or
- (2) go through an incident edge and return to v_i , in which case $\text{sgn}(\gamma) = 1$.

Similarly, an *edge superwalk* of length 1 starting at e_i can

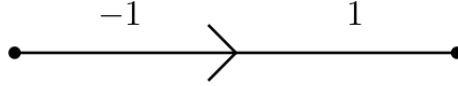
FIGURE 6. Oriented cycle graph C_3 .

- (1) go through an incident vertex v to an adjacent edge e_j , in which case $\text{sgn}(\gamma) = 1$ if e_j and e_i both go into or both leave v and $\text{sgn}(\gamma) = -1$ if one of e_j and e_i enters v and the other exits it, or
- (2) go to an incident vertex and back to e_i in which case $\text{sgn}(\gamma) = 1$.

Similarly, we can define a new type of walk on the graph which is encoded by the Incidence Dirac operator.

Definition 3.13. A *vertex-edge walk* of length 1 moves from a vertex to an incident edge, or an edge to an incident vertex. We can define the sign of the walk as follows: If the edge involved in the walk originates from the vertex involved then $\text{sgn}(\gamma) = -1$ and if the edge enters the vertex involved then $\text{sgn}(\gamma) = 1$. Note for this definition we do not care whether we're starting at a vertex or an edge. For a graphical way of thinking about the signs of these walks see figure 7.

A vertex-edge walk of length k is a combination of k walks of length 1, and has a sign equal to the product of the signs of each step.

FIGURE 7. Signs of vertex-edge walks on a P_2 graph.

By this definition, we note that vertex superwalks are vertex-edge walks with an even length, while edge superwalks are vertex-edge walks of an odd length.

Theorem 3.14.

$$\mathcal{D}_I^k(i, j) = \sum_{\gamma, i \rightarrow j, k} \text{sgn}(\gamma).$$

Proof. We will prove this theorem by induction on k .

Letting $k = 1$, we know $\mathcal{D}_I = \begin{pmatrix} O & I \\ I^t & O \end{pmatrix}$, and checking these entries we see that the theorem is true.

Let it be true for some arbitrary $k - 1$. There are two cases.

Case 1: Let $k - 1$ be odd. Then $\mathcal{D}_I^k = \begin{pmatrix} \Delta_+^{k/2} & O \\ O & \Delta_-^{k/2} \end{pmatrix}$, so we know that the entries count vertex superwalks and edge superwalks of length $k/2$, which means that they count vertex-edge walks of length k .

Case 2: Let $k - 1$ be even. Then $\mathcal{D}_I^k = \begin{pmatrix} O & \Delta_+^{(k-1)/2} I \\ \Delta_-^{(k-1)/2} I^t & O \end{pmatrix}$. We know there cannot be vertex

or edge superwalks, so the 0 block matrices are expected. Because the other block matrices are transposes of one another, we will analyze $A = \Delta_+^{(k-1)/2} I$. Looking at each entry, we have

$$a_{i,j} = \text{row}_i(\Delta_+^{(k-1)/2}) \cdot \text{col}_j(I) = 1 \cdot \sum_{\gamma, i \rightarrow n, k-1} \text{sgn}(\gamma) - 1 \cdot \sum_{\gamma, i \rightarrow m, k-1} \text{sgn}(\gamma),$$

where e_j goes from v_m to v_n . Then because the last step of a vertex-edge walk starting at v_i and ending at e_j must include one of the vertices adjacent to e_j , our sum must include a term for each such walk, and we have that $a_{i,j} = \sum_{\gamma, i \rightarrow j, k} \text{sgn}(\gamma)$. ■

As an example of this result we look to the third power of the incidence matrix for K_3 with clockwise orientation.

$$\mathcal{D}_I^3 = \begin{pmatrix} 0 & 0 & 0 & 0 & 3 & -3 \\ 0 & 0 & 0 & -3 & 0 & 3 \\ 0 & 0 & 0 & 3 & -3 & 0 \\ 0 & -3 & 3 & 0 & 0 & 0 \\ 3 & 0 & -3 & 0 & 0 & 0 \\ -3 & 3 & 0 & 0 & 0 & 0 \end{pmatrix}.$$

Here we see that there are 3 vertex-edge walks between a vertex and an incident edge, and that the powers follow as expected. Looking at the entries between v_1 and e_1 , we see a value of 0, because there are two such walks of length 3 connecting these elements, but these walks have opposite signs, cancelling one another out as seen in Figure 8.

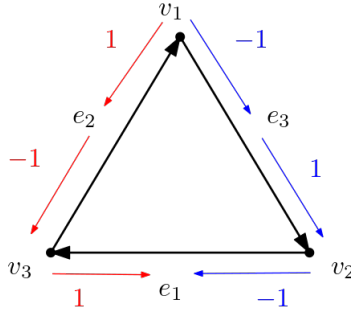


FIGURE 8. Length 3 walks from v_1 to e_1 .

The full list of vertex edge walks and their signs for K_3 originating at v_1 , each of which is equivalent to performing the same moves at one of the other vertices.

$$\begin{array}{ll} \gamma_1 = v_1 \rightarrow e_2 \rightarrow v_3 \rightarrow e_1 & \text{sgn}(\gamma_1) = -1 \\ \gamma_2 = v_1 \rightarrow e_3 \rightarrow v_2 \rightarrow e_1 & \text{sgn}(\gamma_2) = 1 \\ \gamma_3 = v_1 \rightarrow e_2 \rightarrow v_3 \rightarrow e_2 & \text{sgn}(\gamma_3) = 1 \\ \gamma_4 = v_1 \rightarrow e_2 \rightarrow v_1 \rightarrow e_2 & \text{sgn}(\gamma_4) = 1 \\ \gamma_5 = v_1 \rightarrow e_3 \rightarrow v_1 \rightarrow e_2 & \text{sgn}(\gamma_5) = 1 \\ \gamma_6 = v_1 \rightarrow e_3 \rightarrow v_2 \rightarrow e_3 & \text{sgn}(\gamma_6) = -1 \\ \gamma_7 = v_1 \rightarrow e_3 \rightarrow v_1 \rightarrow e_3 & \text{sgn}(\gamma_7) = -1 \\ \gamma_8 = v_1 \rightarrow e_2 \rightarrow v_1 \rightarrow e_3 & \text{sgn}(\gamma_8) = -1. \end{array}$$

4. DIMER MODELS AND A GLUING FORMULA FOR DIRAC OPERATORS

Gluing formulae for discrete operators have been studied in mathematical physics [12], and in the case of the discrete Laplace operator, it has some interesting connections with graph theory [2]. On the other hand, dimer models have been studied extensively in the context of statistical physics, dimer models, quantum mechanics and combinatorics [1, 5, 6].

In this section we describe a combinatorial interpretation of a gluing formula for the Kasteleyn matrix, which can be regarded as a discrete Dirac operator for lattice graphs.

4.1. Graph gluing. First, we define two different types of gluing of graphs, which are relevant while discussing gluing identities for graph Dirac operators.

Definition 4.1. Let Γ_1 and Γ_2 be two graphs. Let Γ_1^∂ and Γ_2^∂ be isomorphic subgraphs of Γ_1 and Γ_2 respectively. Then $I = \Gamma_1^\partial = \Gamma_2^\partial$ is an *interface* of Γ_1 and Γ_2 .

Definition 4.2. Let Γ_1 and Γ_2 be two graphs and I an interface. The *interface gluing* of the two graphs $\Gamma_1 \sqcup_I \Gamma_2$ is defined by: $V(\Gamma_1 \sqcup_I \Gamma_2) = (V(\Gamma_1) \setminus V(I)) \cup (V(\Gamma_2) \setminus V(I)) \cup V(I)$ and $E(\Gamma_1 \sqcup_I \Gamma_2) = (E(\Gamma_1) \setminus V(I)) \cup (E(\Gamma_2) \setminus E(I)) \cup E(I)$.

Definition 4.3. Let Γ_1 and Γ_2 be two graphs. Let $\{v_{1,1}, \dots, v_{1,k}\} \subseteq \Gamma_1$ and $\{v_{2,1}, \dots, v_{2,k}\} \subseteq \Gamma_2$. Let $\{e_1, \dots, e_k\}$ be the set of edges that connect the pairs of vertices $(v_{1,1}, v_{2,1}), \dots, (v_{1,k}, v_{2,k})$. Then a *bridge graph* B between Γ_1 and Γ_2 is the graph with $V(B) = \{v_{1,1}, \dots, v_{1,k}, v_{2,1}, \dots, v_{2,k}\}$ and $E(B) = \{e_1, \dots, e_k\}$.

Definition 4.4. Let Γ_1 and Γ_2 be two graphs and B a bridge graph. The *bridge gluing* of the two graphs $\Gamma_1 \sqcup_B \Gamma_2$ is defined by: $V(\Gamma_1 \sqcup_B \Gamma_2) = V(\Gamma_1) \cup V(\Gamma_2)$ and $E(\Gamma_1 \sqcup_B \Gamma_2) = E(\Gamma_1) \cup E(B) \cup E(\Gamma_2)$.

A *perfect matching* of a graph is a set of edges such that each vertex is connected to exactly one edge. Kasteleyn's Theorem [4] allows us to connect the number of perfect matchings to the Kasteleyn matrix, K , defined as the weighted adjacency matrix of a graph G , with horizontal edges weighted 1 and vertical edges weighted $i = \sqrt{-1}$. We are interested in this matrix because of its connection to graph quantum mechanics: following [6], the matrix K acts like a Dirac operator when restricted to sublattices of a lattice graph. That is, when a lattice graph's Kasteleyn matrix is restricted to the four sublattices comprised of vertices spaced two apart in each cardinal direction, $K^*K = \Delta_+$.

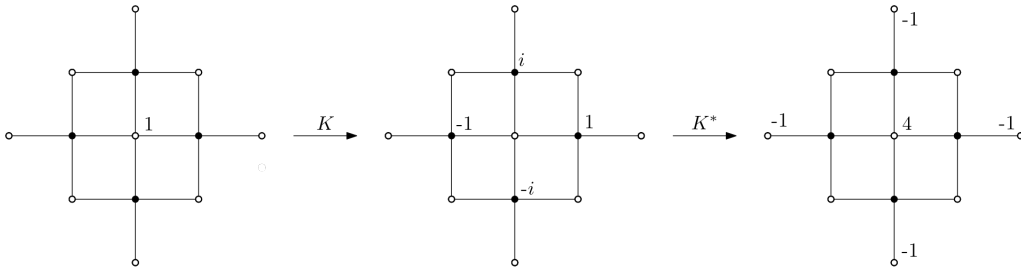


FIGURE 9. Visual representation of Kasteleyn operating on graph as a Laplacian.

We reinterpret Kasteleyn's theorem by introducing explicit recurrence relations for perfect matchings of integer lattices. We prove gluing identities for the determinants of Kasteleyn matrices by introducing explicit formulae for perfect matchings of integer lattices when one of the sides is 2, 3, or 4. We denote an k by n lattice graph as $L_{k,n}$ and the number of ways to tile $L_{k,n}$ as $T_k(n)$.

4.2. The $2 \times n$ case.

Theorem 4.5. *The number of unique ways that dominos can tile $L_{2,n}$ is given by the recursive formula $T_2(n) = T_2(n-1) + T_2(n-2)$, where $T_2(1) = 1$ and $T_2(2) = 2$.*

Proof. For clarity of notation, note that $L_{2,n}$ has 2 rows of vertices and n columns of vertices (so here a vertical domino fills one column of the graph).

We can see that when $n = 1$, $T_2(n) = 1$, as it can only be filled by placing the domino vertically, and when $n = 2$, $T_2(n) = 2$, as it can be filled by placing both tiles vertically or both tiles horizontally. We will now prove that for all $n > 2$, $T_2(n) = T_2(n-1) + T_2(n-2)$.

Let $n > 2$ be arbitrary. We can split the possible ways of filling our graph into 2 cases, depending on the orientation of the tile(s) in the first column

Case 1: Let the first column be filled by a vertically placed domino. Then we have a $L_{2,n-1}$ graph left to fill, so from the definition of our function we have that there are $T_2(n-1)$ unique ways to tile the graph.

Case 2: Let the first 2 columns be filled by 2 horizontally placed dominos. Then we have a $L_{2,n-2}$ graph left to fill, so there will be $T_2(n-2)$ unique ways to tile the graph.

Now because each possible way to fill the graph is given by one of these two cases, $T_2(n)$ will be the sum of the number of ways to fill the graph in each of these cases, so we have that $T_2(n) = T_2(n-1) + T_2(n-2)$. ■



FIGURE 10. Cases for end of a $2 \times n$ graph.

We can also find the formula for the number of perfect matchings for two such graphs glued together. In order to talk about this in more general terms, we will introduce notation for such a formula, given by $T_k(m \sqcup_{s,B} n)$, where we are gluing $L_{k,m}$ and $L_{k,n}$ graphs such that their sides of length k are aligned, with s indicating by how many vertices the right graph has been shifted down relative to the left, as seen in 12, and B being the set of bridges from the gluing included in the perfect matching. s and B aren't extremely impactful in the $2 \times n$ case, but make a big difference with bigger graphs.

Theorem 4.6. *The number of perfect matchings of $L_{2,m}$ and $L_{2,n}$ glued together with a shift is given by*

$$T_2(m \sqcup_{s,B} n) = \begin{cases} T_2(m)T_2(n) & s = 1 \text{ or } 2, B = \emptyset \\ 0 & s = 0 \text{ or } 1, B = \{e_1\} \\ T_2(m)T_2(n) + T_2(m-1)T_2(n-1) & s = 0, B = \emptyset \text{ or } \{e_1, e_2\}. \end{cases}$$

Proof. We begin by noting that in the case of a shift 1 or 2 gluing, it is only possible to tile the graph if we treat them separately, giving rise to the first equation. In general, for $T_k(m \sqcup_{s,B} n)$ where k is even and $|B|$ is odd, we find that there are 0 ways to tile because that would leave an odd number of spaces to tile on either side of the gluing.

For the third case, letting m and n be arbitrary, we want to find how many ways we can tile the $2 \times (m+n)$ graph formed by gluing $2 \times m$ and $2 \times n$ graphs together. We can split this into two sub-cases: that where we include both bridges in the matching and that where neither are included.

Case 1: Let there be no bridges between the graphs. Then for each possible tiling of the $2 \times m$ graph, there are $T_2(n)$ ways to finish the tiling. Thus, in this case there are $T_2(m)T_2(n)$ solutions.

Case 2: Let there be bridges between the graphs. Then we have a $2 \times (m - 1)$ and a $2 \times (n - 1)$ graph left to fill, so there will be $T_2(m - 1)T_2(n - 1)$ solutions. This completes the proof. ■

4.3. The $3 \times n$ case.

Theorem 4.7. *The number of unique ways that dominos can tile $L_{3,n}$ is given by the recursive formula $T_3(n) = 4T_3(n - 2) - T_3(n - 4)$, where $T_3(0) = 1$, $T_3(1) = 0$, $T_3(2) = 3$, and $T_3(3) = 0$.*

Proof. If n is odd, then the total number of spaces is odd, so it is impossible to cover the graph using domino tiles, each of which covers an even number of spaces. In order to have a nonzero number of ways to tile the graph, n must be even, so $n = 2k$ for some $k \in \mathbb{Z}$. Looking at one end of the graph, and considering a vertical line that separates the first two columns from the rest, any tiling will either have no dominoes that cross the line or it will have some dominoes that cross the line. In the first case, there are $T_3(2)T_3(n - 2) = 3T_3(n - 2)$ ways. In the other case, there are some domino tiles that cross the vertical line separating the second and third columns. Now consider a vertical line between the fourth and fifth columns. There are only two ways to tile $L_{3,4}$ with at least one horizontal domino on the second and third columns, adding $2T_3(n - 4)$ ways to tile the whole graph. Similarly, pushing the vertical line further down the graph $2m$ spaces to account for all the possible tilings only adds $2T_3(n - 2m)$ to the total, so the number of ways to tile $L_{3,n}$ is equal to $3T_3(n - 2) + 2(T_3(n - 4) + T_3(n - 6) + \dots + T_3(0))$. Since $2(T_3(n - 4) + T_3(n - 6) + \dots + T_3(0)) = T_3(n - 2) - T_3(n - 4)$, we can simplify $T_3(n)$ to the recurrence relation $T_3(n) = 4T_3(n - 2) - T_3(n - 4)$. ■

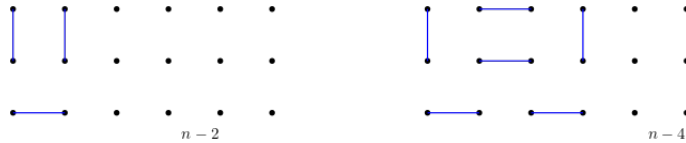


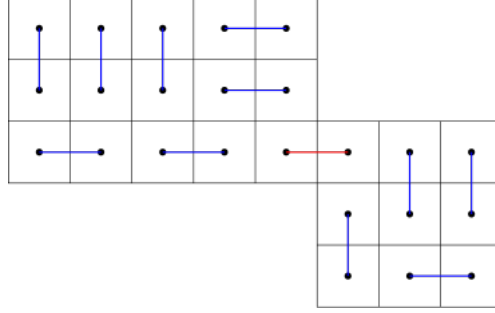
FIGURE 11. First 2 cases for tiling from the end of the graph.

Proposition 4.8.

$$\sum_{i=0}^{\frac{n-2}{2}} T_3(2i) = \frac{T_3(n) - T_3(n - 2)}{2}.$$

Proof. Recall from the proof of 4.7 that $T_3(n) = 3T_3(n - 2) + 2 \sum_{i=0}^{\frac{n-4}{2}} T_3(2i)$. The result follows from subtracting $T_3(n - 2)$ from both sides and dividing by 2. ■

We can also find information about gluing these graphs together, first considering the case where the lattice graphs are shifted such that there is only one bridge between the two, such as in Figure 12.

FIGURE 12. A perfect matching of $L_{3,5} \sqcup_{2,\{e_1\}} L_{3,3}$.

Theorem 4.9. *The number of perfect matchings of $L_{3,m}$ and $L_{3,n}$ glued together with a shift is given by*

$$T_3(m \sqcup_{s,B} n) = \begin{cases} T_3(m)T_3(n) & B = \emptyset \\ \frac{(T_3(m+1)-T_3(m-1))(T_3(n+1)-T_3(n-1))}{4} & s = 2, B = \{e_1\} \\ 0 & s = 1, B = \{e_1\} \text{ or } \{e_2\} \\ \frac{(T_3(m)-T_3(m-2))(T_3(n)-T_3(n-2))}{4} & s = 1, B = \{e_1, e_2\} \\ \frac{(T_3(m+1)-T_3(m-1))(T_3(n+1)-T_3(n-1))}{4} & s = 0, B = \{e_1\} \text{ or } \{e_3\} \\ 0 & s = 0, B = \{e_2\} \text{ or } \{e_1, e_3\} \\ \frac{(T_3(m)-T_3(m-2))(T_3(n)-T_3(n-2))}{4} & s = 0, B = \{e_1, e_2\} \text{ or } \{e_2, e_3\} \\ T_3(m-1)T_3(n-1) & s = 0, B = \{e_1, e_2, e_3\}. \end{cases}$$

Proof. When $B = \emptyset$, there are no bridges between the two lattice graphs, so the number of ways to tile them is the number of ways to tile one of them multiplied by the number of ways to tile the other. That is, $T_3(m)T_3(n)$.

When $s = 2$ and $B = \{e_1\}$ or when $s = 0$ and $B = \{e_1\}$ or $\{e_3\}$, then the graphs are positioned like in Figure 12. If m or n is even, then there will be an odd number of vertices left on either the $3 \times m$ or $3 \times n$ graph which is impossible to tile, so suppose both m and n are odd. The method of solving will be the same for each graph in the gluing, so we will look at the $3 \times n$ graph. On the first row, there are 2 available vertices adjacent to one another, so we can split this into two cases, as seen in Figure 13: either include the vertical edge between the two, in which case there are $T_3(n-1)$ ways to finish the perfect matching, or we include the horizontal edges connecting them to the adjacent row. In this case we're forced to include the edge next to the bridge going into the top or bottom of the third edge. This means we have a $3 \times (n-2)$ lattice graph missing one vertex, so we will finish tiling it in the same way as we tiled the $3 \times n$ graph missing a vertex. Then we will add a $T_3(n-3)$ term and continue until we have a 2×1 graph left, adding $1 = T_3(0)$ to the sum. Thus we get that the number of ways to tile $L_{3,n}$ missing one corner vertex is equal to $T_3(n-1) + T_3(n-3) + \dots + T_3(0)$. By proposition 4.8, this sum equals $\frac{T_3(n+1)-T_3(n-1)}{2}$. Similarly, the number of ways to tile the left graph is $\frac{T_3(m+1)-T_3(m-1)}{2}$. Multiplying these two values together gives us the total number of tilings for these shift and bridge gluing combinations: $\frac{(T_3(m+1)-T_3(m-1))(T_3(n+1)-T_3(n-1))}{4}$.

When $s = 1$ and $B = \{e_1\}$ or $\{e_2\}$ or when $s = 0$ and $B = \{e_2\}$ or $\{e_1, e_3\}$, then at least one of the $3 \times m$ or the $3 \times n$ graph will have either only the middle tile or only the top and bottom tiles of an end column covered, as in Figure 14, which is impossible to tile. This is because the only way to fill the top and bottom spaces of an end column missing its middle tile is with horizontal

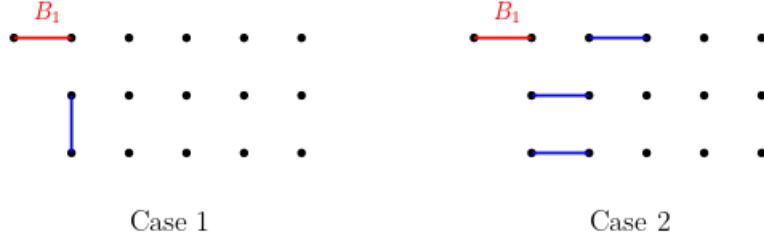


FIGURE 13. Possible ways to finish a perfect matching including B_1 .

tiles, which then leaves the middle tile of the second column uncovered in a way that can only be covered by a horizontal tile. However, once that space has been covered, the graph is in the same state as it was at the beginning, though now two of its columns have been covered. This process repeats itself, forcing the placement of horizontal tiles until there is not enough space for another domino and either the middle vertex or the top and bottom vertices of the end column will always be uncovered, meaning there is no way to tile the whole graph. Therefore, these combinations of shifting and gluing contribute 0 to the total.

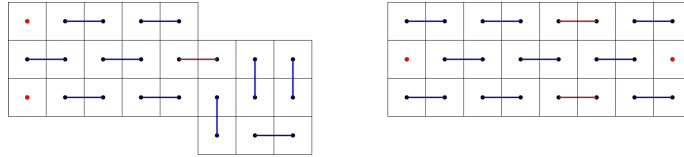


FIGURE 14. Impossible tiling configurations.

When $s = 1$ and $B = \{e_1, e_2\}$ or when $s = 0$ and $B = \{e_1, e_2\}$ or $\{e_2, e_3\}$, then the graphs are positioned like in Figure 15. If m or n is odd, then there will be an odd number of spaces left on either the $3 \times m$ or $3 \times n$ graph which is impossible to tile, so suppose both m and n are even. Then for each graph we have an odd number of rows with one extra tile, forcing us to place a domino horizontally next to the bridges. This leaves a $3 \times (m - 1)$ graph missing a vertex to fill. In the proof of the $s = 2$ and $B = \{e_1\}$ or when $s = 0$ and $B = \{e_1\}$ or $\{e_3\}$ gluing cases we showed that the number of ways to finish tiling such a graph is given by $\frac{T_3(m)-T_3(m-2)}{2}$, so in this case the total number of ways to tile the graph is given by multiplying this result for m with the same result for n . Adding these formulas together gives us the final result: $\frac{(T_3(m)-T_3(m-2))(T_3(n)-T_3(n-2))}{4}$.

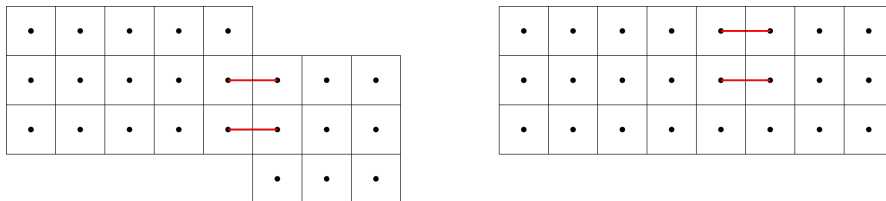


FIGURE 15. Initial tiling configurations of $L_{3,5} \sqcup_{1, \{e_1, e_2\}} L_{3,3}$ and $L_{3,5} \sqcup_{0, \{e_1, e_2\}} L_{3,3}$.

When $s = 0$ and $B = \{e_1, e_2, e_3\}$, then the graphs are positioned like in Figure 16. This configuration leaves a $3 \times (m - 1)$ and a $3 \times (n - 1)$ graph to be tiled, so the number of ways to

tile them is the number of ways to tile one of them multiplied by the number of ways to tile the other. That is, $T_3(m-1)T_3(n-1)$.

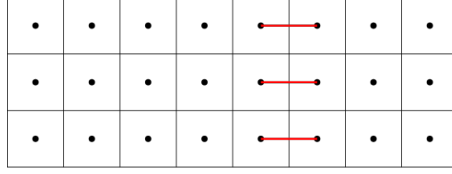


FIGURE 16. Initial tiling configuration of $L_{3,5} \sqcup_{0, \{e_1, e_2, e_3\}} L_{3,3}$.

■

In the proof for Theorem 4.9, the cases for the number of perfect matchings were split based on the shift and bridges that defined the gluing. We can combine a number of these cases to express $T_3(m+n)$ in terms of tilings relating to m and n (See Corollary A.1).

4.4. The $4 \times n$ case.

Theorem 4.10. *The number of unique ways to tile $L_{4,n}$ with dominoes is given by the recursive formula $T_4(n) = T_4(n-1) + 5T_4(n-2) + T_4(n-3) - T_4(n-4)$, where $T_4(1) = 1$, $T_4(2) = 5$, $T_4(3) = 11$, and $T_4(4) = 36$.*

Proof. The initial values of the recursion can be checked by hand. As for the recursive formula, let n be an arbitrary positive integer greater than 4. All possible tilings of $L_{4,n}$ must begin on the left-hand side with one of these initial configurations:

In the first case, where the first column is filled with vertical dominoes, there is a $4 \times (n-1)$ graph left to tile, contributing $T_4(n-1)$ ways to fill the graph.

In the second case, where the first two columns are filled with horizontal dominoes, there is a $4 \times (n-2)$ graph left to tile, contributing $T_4(n-2)$ ways to fill the graph.

In the third case, the two empty spaces in the second column can either be filled with a vertical tile or two horizontal tiles. Adding a vertical tile leaves a $4 \times (n-2)$ graph to tile and adding two horizontal tiles gives you the same choice of filling the two empty spaces in the third column either by adding a vertical tile or two horizontal tiles. You can continue choosing to add horizontal tiles until you run out of space on the graph, in total adding $T_4(n-2) + T_4(n-3) + T_4(n-4) + \dots + T_4(0) = \sum_{i=0}^{n-2} T_4(i)$ ways to tile the graph. The same goes for the fourth case.

In the fifth case, the two empty spaces in the second column can either be filled with a vertical tile or two horizontal tiles. Adding a vertical tile leaves a $4 \times (n-2)$ graph to tile and adding two horizontal tiles forces you to place horizontal tiles in the top and bottom rows and then gives you the same choice of filling the two empty spaces in the fourth column either by adding a vertical tile or two horizontal tiles. You can continue choosing to add horizontal tiles until you run out of space on the graph, in total adding

$$T_4(n-2) + T_4(n-4) + T_4(n-6) + \dots + ((T_4(1) \text{ if } n \text{ is odd}) \text{ or } (T_4(0) \text{ if } n \text{ is even})) = \sum_{i=1}^{\lfloor \frac{n}{2} \rfloor} T_4(n-2i)$$

ways to tile the graph.

So far, we have

$$T_4(n) = T_4(n-1) + T_4(n-2) + 2 \sum_{i=0}^{n-2} T_4(i) + \sum_{i=1}^{\lfloor \frac{n}{2} \rfloor} T_4(n-2i).$$

However, we can simplify this formula further:

$$T_4(n-2) = T_4(n-3) + T_4(n-4) + 2 \sum_{i=0}^{n-4} T_4(i) + \sum_{i=1}^{\lfloor \frac{n-2}{2} \rfloor} T_4(n-2-2i),$$

so

$$\begin{aligned} T_4(n) - T_4(n-2) &= (T_4(n-1) + T_4(n-2) + 2 \sum_{i=0}^{n-2} T_4(i) + \sum_{i=1}^{\lfloor \frac{n}{2} \rfloor} T_4(n-2i)) \\ &\quad - (T_4(n-3) + T_4(n-4) + 2 \sum_{i=0}^{n-4} T_4(i) + \sum_{i=1}^{\lfloor \frac{n-2}{2} \rfloor} T_4(n-2-2i)) \\ &= T_4(n-1) + 4T_4(n-2) + T_4(n-3) - T_4(n-4) \end{aligned}$$

So $T_4(n) = T_4(n-1) + 5T_4(n-2) + T_4(n-3) - T_4(n-4)$. ■

In order to prove a gluing formula for the $4 \times n$ case, it will be helpful to derive formulae for the sums in the proof of the recursion formula, see Propositions A.3 and A.4 in the Appendix.

We can also find information about gluing graphs together, considering different shifts and bridge sets. If the number of bridges is odd, then what it left is impossible to tile because an odd number of vertices will be left on each graph.

Theorem 4.11. *The number of perfect matchings of $L_{4,m}$ and $L_{4,n}$ glued together with a shift $T_4(m \sqcup_{s,B} n)$ is given by*

$$\left\{ \begin{array}{ll} T_4(m)T_4(n) & B = \emptyset \\ \frac{(T_4(m+1)-T_4(m-2))(T_4(n+1)-T_4(n-2))}{25} & s = 2, B = \{e_1, e_2\} \\ f(m) \frac{(T_4(n+1)-T_4(n-2))}{5} & s = 1, B = \{e_1, e_2\} \\ \frac{(T_4(m+1)-T_4(m-2))}{5} f(n) & s = 1, B = \{e_2, e_3\} \\ \frac{(T_4(m+1)-T_4(m-2))(T_4(n+1)-T_4(n-2))}{25} & s = 0, B = \{e_1, e_2\} \text{ or } \{e_3, e_4\} \\ 0 & s = 0 \text{ or } 1, B = \{e_1, e_3\} \text{ or } \{e_2, e_4\} \\ f(m+1)f(n+1) & s = 0, B = \{e_1, e_4\} \\ f(m)f(n) & s = 0, B = \{e_2, e_3\} \\ T_4(m-1)T_4(n-1) & s = 0, B = \{e_1, e_2, e_3, e_4\} \end{array} \right.$$

Where $f(n) = -\frac{2}{5}T_4(n) + 4T_4(n-2) + \frac{7}{5}T_4(n-3) - T_4(n-4)$.

Proof. When $B = \emptyset$, there are no bridges between the two lattice graphs, so the number of ways to tile them is the number of ways to tile one of them multiplied by the number of ways to tile the other. That is, $T_4(m)T_4(n)$.

When $s = 2$ and $B = \{e_1, e_2\}$ or when $s = 0$ and $B = \{e_1, e_2\}$ or $\{e_3, e_4\}$, then the graphs are positioned like in Figure 17. The method of solving will be the same for each graph in the gluing, so we will look at the $4 \times n$ graph. On the first row, there are 2 available vertices adjacent to one another, so we can split this into two cases as shown in 18: either include the vertical edge between the two, in which case there are $T_4(n-1)$ ways to finish the perfect matching, or we include the horizontal edges connecting them to the adjacent row. In this case we again have the choice between including a vertical edge, leaving us with a $4 \times (n-2)$ graph to tile, adding $T_4(n-2)$ ways to finish the perfect matching, or including two horizontal edges, again allowing for either a vertical tile or two horizontal tiles. This will continue until we have a 2×1 graph left, adding $1 = T_4(0)$

to the sum. Thus we get that the number of ways to tile $L_{4,n}$ missing one corner vertex and one vertex above or beneath it is equal to $T_4(n-1) + T_4(n-2) + \dots + T_4(0)$. By proposition A.3, this sum equals $\frac{T_4(n+1)-T_4(n-2)}{5}$. Similarly, the number of ways to tile the left graph is $\frac{T_4(m+1)-T_4(m-2)}{5}$. Multiplying these two values together gives us the total number of tilings for these shift and bridge gluing combinations: $\frac{(T_4(m+1)-T_4(m-2))(T_4(n+1)-T_4(n-2))}{25}$.

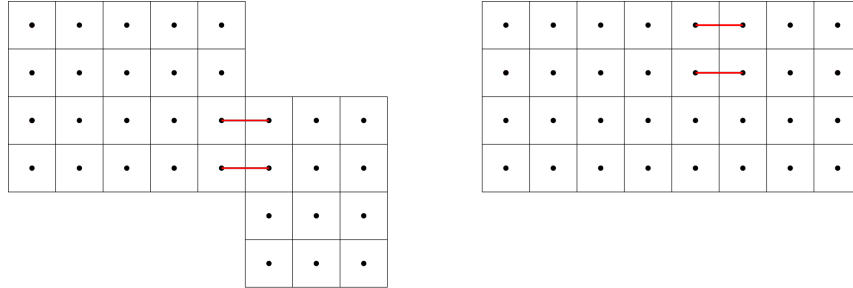


FIGURE 17. Initial tiling configurations of $L_{4,5} \sqcup_{2,\{e_1,e_2\}} L_{4,3}$ and $L_{4,5} \sqcup_{0,\{e_1,e_2\}} L_{4,3}$.

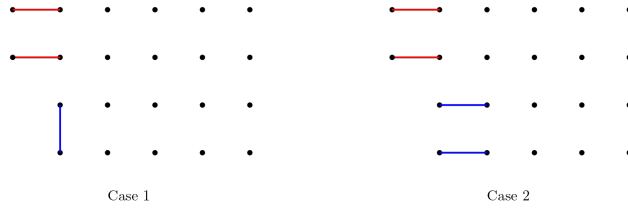


FIGURE 18. Intermediate tiling configurations of $L_{4,5}$ glued with 2 bridges.

When $s = 1$ and $B = \{e_1, e_2\}$ or $\{e_2, e_3\}$, then the graphs are positioned like in Figure 19. This means that one of the graphs will be missing one corner vertex and another vertex above or beneath the corner and the other graph will be missing the middle two vertices from one of the end columns. We already have a formula from the previous paragraph for the number of perfect matchings of the first graph, so let us focus on the second. Since the middle two vertices of the end column are covered, we are forced to place two horizontal tiles on the corner spaces. To fill the second-to-last column, we can either use a vertical tile or two horizontal tiles, as shown in Figure 19. In the case of a vertical tile, we are left with a $4 \times (m-2)$ graph, contributing $T_4(m-2)$ perfect matchings to the total. In the case of two horizontal tiles, we are again forced to place horizontal tiles in the top and bottom rows, now leaving the middle two vertices of the fourth column uncovered, and thus the pattern repeats, adding $T_4(m-2k)$ (where $1 \leq k \leq \lfloor \frac{m}{2} \rfloor$) tilings in each iteration until there is either the middle two vertices of the last column or the entire last column and the middle two vertices of the second-to-last column left uncovered, depending on if m is even or odd. Therefore, in total there are

$$\begin{aligned} & T_4(m-2) + T_4(m-4) + T_4(m-6) + \dots + (T_4(1) \text{ if } m \text{ is odd) or } (T_4(0) \text{ if } m \text{ is even}) \\ &= \sum_{i=1}^{\lfloor \frac{m}{2} \rfloor} T_4(m-2i) = -\frac{2}{5}T_4(m) + 4T_4(m-2) + \frac{7}{5}T_4(m-3) - T_4(m-4) \end{aligned}$$

ways to tile $L_{4,m}$ with the middle two vertices missing from the last column. From now on, we will abbreviate this quantity as $f(m)$. By multiplying this value by the number of ways to tile $L_{4,n}$ missing a corner vertex and a vertex directly below it, we see that there are

$$f(m) \frac{(T_4(n+1) - T_4(n-2))}{5}$$

ways to tile two lattice graphs shifted by 1 with a bridge set equal to $\{e_1, e_2\}$ and

$$\frac{(T_4(m+1) - T_4(m-2))}{5} f(n)$$

ways to tile two lattice graphs shifted by 1 with a bridge set equal to $\{e_2, e_3\}$.

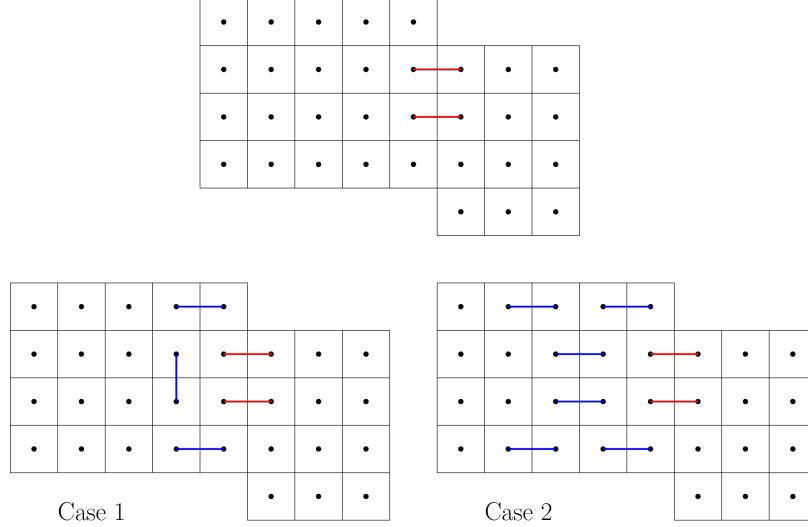
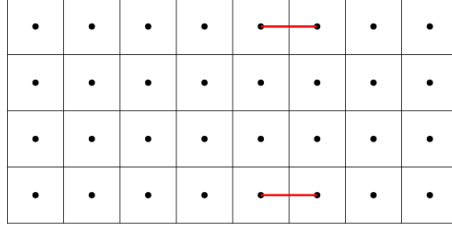


FIGURE 19. Initial and intermediate tiling configurations of $L_{4,5} \sqcup_{1, \{e_1, e_2\}} L_{4,3}$.

When $s = 0$ or 1 and $B = \{e_1, e_3\}$ or $\{e_2, e_4\}$, then at least one of the graphs has its corner vertex missing along with a non corner, nonadjacent vertex from the same column, which is impossible to tile. This is because the only way to cover the vertices of an end column missing a corner and a non corner, nonadjacent tile is with horizontal tiles, which then leaves two nonadjacent vertices of the second column uncovered in a way that can only be covered by two more horizontal tiles. However, once those vertices have been covered, the graph is in the same state as it was at the beginning, though now two of its columns have been covered. This process repeats itself, forcing the placement of horizontal tiles until there is no more space on the graph and either the middle vertex or the top and bottom vertices of the end column will always be uncovered, meaning there is no way to tile the whole graph. Therefore, these combinations of shifting and gluing contribute 0 to the total.

When $s = 0$ and $B = \{e_1, e_4\}$, then we have two graphs next to each other, each missing two corner vertices from an end column, as shown in Figure 20. We will look at just the right graph, since the possible ways to tile each graph are the same. We can either use one vertical tile or two horizontal tiles to cover the vertices in the column missing its corners. If we use a vertical tile, there are $T_4(n-1)$ ways to tile the $4 \times (n-1)$ graph that remains. If we use two horizontal tiles, we are forced to place two more horizontal tiles in the top and bottom rows, so what's left is a $4 \times (n-2)$ graph with two of the corners missing from the left-most column. As we have seen before, we can keep reducing the length of the graph like this, adding $T_4(n-2k+1)$ (where $1 \leq k \leq \lfloor \frac{n}{2} \rfloor$) perfect matchings to the total with each iteration until there is either the middle two vertices of the last column or the entire last column and the middle two vertices of the second-to-last column left uncovered, depending on if n is even or odd. Therefore, in total there are $T_4(n-1) + T_4(n-3) + T_4(n-5) + \dots + (T_4(1)$ if n is even) or $(T_4(0)$ if n is odd) $= \sum_{i=1}^{\lfloor \frac{n}{2} \rfloor} T_4(n-2i+1)$, which, by Proposition A.4 equals $f(n+1)$ ways to tile $L_{4,n}$ with the two corner vertices missing from the last column. The number of ways to tile the left graph is the same except for replacing every instance of n with m . By multiplying these values together, we see that there are $f(n+1)f(m+1)$ ways to tile two lattice graphs shifted by 0 with a bridge set equal to $\{e_1, e_4\}$.

FIGURE 20. Initial tiling configuration of $L_{4,5} \sqcup_{0, \{e_1, e_4\}} L_{4,3}$.

When $s = 0$ and $B = \{e_2, e_3\}$, then we have two graphs next to each other, each missing the two middle vertices from their end columns. From a previous paragraph, we know there are

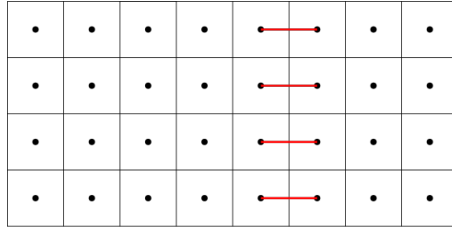
$$-\frac{2}{5}T_4(m) + 4T_4(m-2) + \frac{7}{5}T_4(m-3) - T_4(m-4)$$

ways to tile such graphs. By multiplying these values together, we see that there are

$$f(m)f(n)$$

ways to tile two lattice graphs shifted by 0 with a bridge set equal to $\{e_2, e_3\}$.

When $s = 0$ and $B = \{e_1, e_2, e_3, e_4\}$, then the graphs are positioned like in Figure 21. This configuration leaves a $4 \times (m-1)$ and a $4 \times (n-1)$ graph to be tiled, so the number of ways to tile them is the number of ways to tile one of them multiplied by the number of ways to tile the other. That is, $T_4(m-1)T_4(n-1)$.

FIGURE 21. Initial tiling configuration of $L_{4,5} \sqcup_{1, \{e_1, e_2, e_3, e_4\}} L_{4,3}$.

■

5. SPINORS, CLIFFORD ALGEBRAS ON GRAPHS AND GLUING

Spinors can be examined as elements of linear representation of Clifford Algebras. For example, the space of Pauli spinors can be approached as the space $Cl^-(0, 3)$ and the space of Dirac spinors as $Cl^+(1, 3)$ [11]. The relations between the generators of the algebra parallel the rules governing interactions between spinors in a quantum system. While there are a number of candidate Clifford algebras that have been explored as representations of the space of spinors [11], we focus on a special type of Clifford algebra associated to a graph, introduced by Khovanova [7].

Definition 5.1. Let Γ be a graph with n vertices. Its associated Clifford algebra A_Γ has n generators e_1, \dots, e_n corresponding to each vertex. For each i , $e_i^2 = -1$ and

$$\begin{cases} e_i e_j = -e_j e_i & i \text{ and } j \text{ are adjacent in } \Gamma \\ e_i e_j = e_i e_j & i \text{ and } j \text{ not adjacent in } \Gamma \end{cases}$$

The center of a Clifford graph algebra characterizes the structure of the whole algebra. Each central monomial of a Clifford graph algebra gives a decomposition as a direct sum of two algebras. As a result, the structure of a Clifford graph algebra can be identified solely by the number of vertices and the dimension of its center [7].

The center of a Clifford graph algebra is spanned by its monomials. They are determined by the structure of the graph [7], as stated in the following

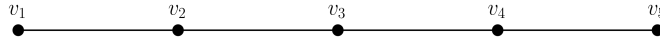
Lemma 5.2. A monomial e_α is central if and only if for each vertex $i \in \Gamma$, there are an even number of edges connecting i to α .

5.1. **Examples.** We give some examples of Clifford graph algebras and their centers.

Proposition 5.3. Let P_n be a path graph. Then

$$Z(A_{P_n}) = \begin{cases} \mathbb{C} & \text{if } n \text{ is even} \\ \mathbb{C}^2 & \text{if } n \text{ is odd} \end{cases}.$$

To be precise, for odd n , $Z(A_{P_n})$ is spanned by the central monomial $e_1 e_3 \cdots e_n$ and 1. Consider the path graph P_5 , labeled as follows:



The center of P_7 is $Z(A_{P_7}) = \{\alpha e_1 e_3 e_5 + \beta \mid \alpha, \beta \in \mathbb{C}\}$.

$e_1 e_3 e_5$ is a central monomial in A_{P_7} because we can check that each vertex is connected to $\alpha = \{1, 3, 5\}$ by an even number of edges.

All edges in P_5 connect an even vertex to an odd vertex. This means for odd i , there are no edges connecting it to α . For even i , the only incident edges are $(i, i-1)$ and $(i, i+1)$. Both $i-1$ and $i+1$ are in α , so there are two edges connecting it to α .

5.2. **Graph gluing and Clifford algebras.**

Definition 5.4. Let V, W be two \mathbb{C} -algebras with bases $\{v_i\}_{i=1}^n$ and $\{w_j\}_{j=1}^m$. The tensor product $V \otimes W$ has basis $\{v_i \otimes w_j\}$ such that

- (1) $(v_1 + v_2) \otimes w = v_1 \otimes w + v_2 \otimes w$
- (2) $v \otimes (w_1 + w_2) = v \otimes w_1 + v \otimes w_2$
- (3) $\lambda(v \otimes w) = (\lambda v) \otimes w = v \otimes (\lambda w), \lambda \in \mathbb{C}$.

In the case of Clifford graph algebras: V and W are \mathbb{C} -algebras spanned by monomials. Assume the generators $\{e_k\}$ for V are distinct from the generators $\{e_l\}$ for W . Each element $v \in V$ and $w \in W$ is a polynomial:

- (1) $v = \sum_{i=1}^n \alpha_i v_i$
- (2) $w = \sum_{j=1}^m \lambda_j w_j$,

where $\alpha_i, \lambda_j \in \mathbb{C}$. Following the normal rules of multiplying two monomials, we define the tensor product $v_i \otimes w_j = v_i w_j$. Because the monomial v_i is defined in different generators from w_j , $v_i w_j$ is a monomial of degree 1.

Under the normal polynomial multiplication, we have:

$$v \otimes w = vw = \sum_{i=1}^n \sum_{j=1}^m \alpha_i \lambda_j v_i w_j.$$

Every element $v \otimes w \in V \otimes W$ is a linear combination of the monomials $v_i \otimes w_j = v_i w_j$. In addition, polynomial multiplication satisfies the following properties:

- (1) $(v_1 + v_2)w = v_1w + v_2w \iff (v_1 + v_2) \otimes w = v_1 \otimes w + v_2 \otimes w$
- (2) $v(w_1 + w_2) = vw_1 + vw_2 \iff v \otimes (w_1 + w_2) = v \otimes w_1 + v \otimes w_2$
- (3) $\lambda vw = (\lambda v)w = v(\lambda w) \iff \lambda(v \otimes w) = (\lambda v) \otimes w = v \otimes (\lambda w)$.

Theorem 5.5. *Let Γ_1 and Γ_2 be graphs and A_{Γ_1} and A_{Γ_2} be their associated Clifford algebras. Then $Z(A_{\Gamma_1}) \otimes Z(A_{\Gamma_2}) = Z(A_{\Gamma_1 \sqcup \Gamma_2})$.*

Proof. (\Rightarrow) First, we need to show $Z(A_{\Gamma_1}) \otimes Z(A_{\Gamma_2}) \subseteq Z(A_{\Gamma_1 \sqcup \Gamma_2})$.

Let $\{e_\alpha\}$ be the basis of central monomials for $Z(A_{\Gamma_1})$ and $\{e_\beta\}$ be the basis of central monomials for $Z(A_{\Gamma_2})$.

Then $\{e_\alpha e_\beta\}$ is a basis for $Z(A_{\Gamma_1 \sqcup \Gamma_2})$. We want to show it is contained in $Z(A_{\Gamma_1} \sqcup A_{\Gamma_2})$.

Let $e_\alpha e_\beta$ be fixed. Observe $e_\alpha e_\beta$ is a monomial associated with the vertex set $\alpha \sqcup \beta$, so we can denote $e_{\alpha\beta} = e_\alpha e_\beta$.

Recall a monomial e_α is central in A_Γ if and only if for all $v \in V(\Gamma)$, the number of edges connecting it to α is even.

In order to show $e_{\alpha\beta} \in Z(A_{\Gamma_1 \sqcup \Gamma_2})$, we need to show for every $v \in V(\Gamma_1 \sqcup \Gamma_2)$, there are an even number of edges connecting it to $\alpha \sqcup \beta$.

Case 1: $v \in V(\Gamma_1)$. Because e_α is a central monomial of A_{Γ_1} , there are an even number of edges connected v to α . Γ_1 and Γ_2 are disconnected in $\Gamma_1 \sqcup \Gamma_2$, so there are no edges between v and β .

Together, there are an even number of edges connecting v to $\alpha \sqcup \beta$.

Case 2: $v \in V(\Gamma_2)$. Because e_β is a central monomial of A_{Γ_2} , there are an even number of edges connected v to β .

Γ_1 and Γ_2 are disconnected in $\Gamma_1 \sqcup \Gamma_2$, so there are no edges between v and α .

Together, there are an even number of edges connecting v to $\alpha \sqcup \beta$.

We thus conclude that $e_\alpha e_\beta = e_{\alpha\beta}$ is a central monomial of $A_{\Gamma_1 \sqcup \Gamma_2}$. It follows that $Z(A_{\Gamma_1}) \otimes Z(A_{\Gamma_2}) \subseteq Z(A_{\Gamma_1 \sqcup \Gamma_2})$.

(\Leftarrow) Next, we need to show $Z(A_{\Gamma_1 \sqcup \Gamma_2}) \subseteq Z(A_{\Gamma_1}) \otimes Z(A_{\Gamma_2})$.

Let $\{e_\alpha\}$ be the basis of monomials for $Z(A_{\Gamma_1 \sqcup \Gamma_2})$. We want to show it is contained in $Z(A_{\Gamma_1}) \otimes Z(A_{\Gamma_2})$.

Let e_α be a central monomial of $A_{\Gamma_1 \sqcup \Gamma_2}$. Because Γ_1 and Γ_2 are disconnected components of $\Gamma_1 \sqcup \Gamma_2$, we can separate the vertex set $\alpha = \alpha_1 \sqcup \alpha_2$, where α_1 and α_2 are the subsets of vertices from Γ_1 and Γ_2 , respectively.

We want to show $e_\alpha = e_{\alpha_1} e_{\alpha_2} \in Z(A_{\Gamma_1}) \otimes Z(A_{\Gamma_2})$, or $e_{\alpha_1} \in Z(A_{\Gamma_1})$ and $e_{\alpha_2} \in Z(A_{\Gamma_2})$.

Start with e_{α_1} . Let $v \in V(\Gamma_1)$.

Because e_α is a central monomial of $\Gamma_1 \sqcup \Gamma_2$, we know there are an even number of edges between v and $\alpha_2 \sqcup \alpha_2$. In particular, there are no edges between v and α_2 because Γ_1 and Γ_2 are disconnected. Then the number of edges connecting v to α_1 is the same for $\alpha_1 \sqcup \alpha_2$, which is even. We have shown for any $v \in V(\Gamma_1)$, there are an even number of edges connecting it to α_1 , so e_{α_1} is a central monomial of A_{Γ_1} . Similarly, we can find that e_{α_2} is a central monomial of A_{Γ_2} . Then $e_\alpha = e_{\alpha_1} e_{\alpha_2} \in Z(A_{\Gamma_1}) \otimes Z(A_{\Gamma_2})$. We conclude $Z(A_{\Gamma_1 \sqcup \Gamma_2}) \subseteq Z(A_{\Gamma_1}) \otimes Z(A_{\Gamma_2})$, as desired. \blacksquare

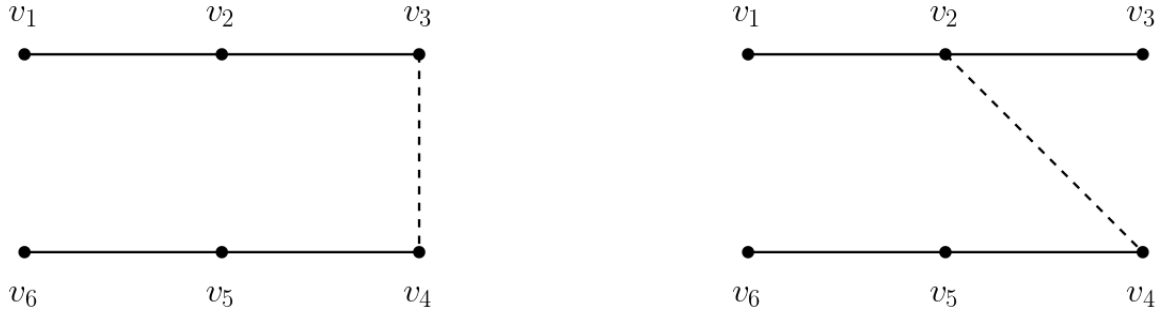
The centers of Clifford graph algebras from bridge gluings are more challenging to identify, but we can start with some simple examples.

There are two ways to glue the path graphs P_2 and P_3 with one bridge:

By Proposition 5.3, the bases for $Z(A_{P_2})$ and $Z(A_{P_3})$ are $\{1\}$ and $\{1, e_1 e_3\}$, respectively. In the left gluing, $P_2 \sqcup_{B_1} P_3 = P_5$, which has a center spanned by $e_1 e_3 e_5$ and 1. The right gluing also has basis $\{e_1 e_3 e_5, 1\}$. With the same number of vertices and dimension of their centers, the Clifford algebras associated to the two bridge gluings are isomorphic.

FIGURE 22. Two different bridge gluings between P_3 and P_2 .

This is not always the case though. Take the following gluing of two copies of P_3 :

FIGURE 23. Two different bridge gluings between two copies of P_3 .

The Clifford algebra of the left gluing has a center of dimension one, while the center for the right gluing has dimension four with central monomials e_1e_3 , $e_1e_4e_6$, and $e_3e_4e_6$.

We can characterize the dimension of the Clifford algebras of glued path graph. The case of bridge gluing the endpoints of two path graphs is simple: by Proposition 5.3, $P_n \sqcup_{B_1} P_m$ has a center of dimension 1 if n and m have the same parity and 0 if they have opposite parity.

Theorem 5.6. *Let $\Gamma = P_n \sqcup_{B_1} P_m$ be two path graphs glued by a bridge between an interior vertex and endpoint.*

- (1) *If n and m are both even, then $Z(A_\Gamma)$ has dimension 1.*
- (2) *If n is even and m is odd, then $Z(A_\Gamma)$ has dimension 2.*
- (3) *If n and m are both odd, then $Z(A_\Gamma)$ has dimension 4.*

We prove the following lemma to identify central monomials of the glued graph Clifford algebra:

Lemma 5.7. Let Γ be a tree. Suppose e_α is a central monomial of A_Γ . Then

- (1) there are at least one vertex of degree one in α ,
- (2) for every vertex $v \in \alpha$, there exists $u \in \alpha$ such that $d(u, v) = 2$, and
- (3) no pair of vertices $u, v \in \alpha$ are adjacent.

This will help us to prove Theorem 5.6, because we only need to check the vertex sets that start at a leaf and skip every other vertex.

Proof. Let e_α be a central monomial of A_Γ .

- (1) Suppose for the sake of contradiction, there is no vertex of degree one in α .

Pick any interior vertex of Γ as the root r . This gives Γ a partial ordering relation $<_r$, where $x <_r y$ if x lies in the $r - y$ path. Pick any maximal element $x \in \alpha$, that is, there is no $y \in \alpha$ such that $x <_r y$. By assumption, x is not a leaf, so there is some vertex v that is adjacent to x away from the root r . Then v is connected to α by a single edge (v, x) . There

are no other edges between v and α because for any other neighbor u , $x <_r u$, so $u \notin \alpha$ by the maximality of x . We conclude e_α is not a central monomial, in contradiction.

- (2) Let $v \in \alpha$. Suppose for the sake of contradiction, there is no vertex $u \in \alpha$ such that $d(u, v) = 2$. Pick any vertex x adjacent to v . Then x is connected to α by a single edge (v, x) . There are no other edges between x and α because for any other neighbor y , $d(y, v) = 2$. We conclude e_α is not a central monomial, in contradiction.

- (3) Let $v \in \alpha$. Suppose for sake of contradiction, $u, v \in \alpha$ that are adjacent.

Case 1: u or v is a leaf. Assume WLOG v is a leaf. Then v is connected to α by a single edge (u, v) , since v has no other neighbors.

Case 2: u and v are both interior vertices. At least one neighbor of v , say x , is in α , otherwise v only has one edge connecting it to α . We can show the same for x , at least one of its neighbors is in α . We repeat until we have found some leaf z in α , which is connected to α by a single edge. In contradiction, e_α is not a central monomial. ■

One corollary of this proof is that if a central vertex set starts at one leaf, then branches out, skipping every other vertex, then it must contain a leaf at the end of the branch. Otherwise, like in part 1, the “next” vertex in the branch connects to the vertex set by one edge. As a result, the vertex set corresponding to a central monomial must contain at least two leaves that are an even distance apart.

Now we are able to prove Theorem 5.6.

Proof. Let P_n and P_m be two path graphs. Label the vertices of P_n , v_1, \dots, v_n , and similarly for P_m . Let Γ be P_n and P_m glued by bridge (v_k, u_1) , where v_k is an internal vertex of P_n and u_1 is an endpoint of P_m .

Case 1: n and m are both even.

Because n is even, we know v_k is an even distance from some endpoint of P_n and an odd distance from the other. Assume WLOG v_k is an even distance from v_1 . The only pair of leaves that are an even apart is v_1 and u_1 , so any central vertex set must contain $v_1, \dots, v_k, u_2, \dots, u_m$. We note v_{k-1} connects to the set by a single edge (v_{k-1}, v_k) , so its associated monomial is not central. However, if it branches towards v_{k-2} from v_k , it will not contain leaf v_1 because they are odd distances apart.

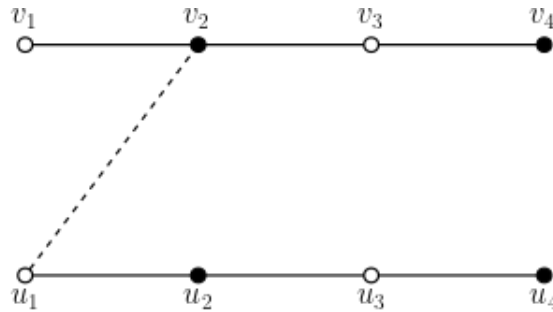
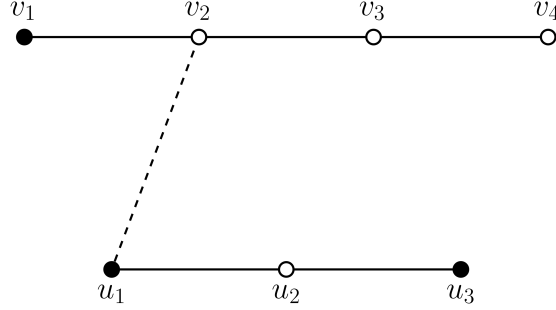


FIGURE 24. A candidate vertex set

Case 2: n is even and m is odd.

Let's assume without loss of generality that v_k is at an even distance from v_1 . We observe $v_1, \dots, v_k, u_2, \dots, u_m$ corresponds to a central monomial. Moreover, this is the only central monomial because the other pairs of leaves are an odd distance apart.

FIGURE 25. The vertex set associated to the unique central monomial of A_Γ

Case 3: n is odd and m is even.

Because n is odd, v_{nk} is either an odd distance from both endpoints or an even distance from both endpoints of P_n .

Suppose v_{nk} is an even distance from both v_{n1} and v_{nn} . Then $v_{n1}, \dots, v_{nk}, \dots, v_{nn}, v_{m2}, \dots, v_{mm}$.

If v_{nk} is an odd distance from both v_{n1} and v_{nn} , then it is equivalent to Case 2. Γ is also two paths, $v_1, \dots, v_k, u_1, \dots, u_m$ and v_{k+1}, \dots, v_n , glued by bridge (v_k, v_{k+1}) . The former has an even number of vertices while the latter has an odd number, like in Case 2.

Case 4: n and m both odd.

Assume k is even. Otherwise, if k is odd, Γ can also be seen as two paths, $v_{n1}, \dots, v_{nk}, v_{m1}, \dots, v_{mm}$ and $v_{n(k+1)}, \dots, v_{nn}$ glued by bridge $(v_{nk}, v_{n(k+1)})$. Both path graphs have even length, as in Case 1.

The vertex sets associated to central monomials are:

- $v_1, \dots, v_{k-1}, v_{k+1}, \dots, v_n$
- $v_1, \dots, v_{k-1}, u_1, \dots, u_m$
- $v_n, \dots, v_{k+1}, u_1, \dots, u_m$.

■

6. FUTURE DIRECTIONS

Currently, our program to compute and create visualizations of solutions to the Dirac equation over time has been used to numerically verify our results. Future directions include investigating whether this process can be carried out in reverse, i.e. can information about the underlying graph or initial quantum state be extracted given these graphs and data of solutions to the Dirac equation over time.

Our gluing formulae help us to understand the behavior of spinors and Dirac operators on graphs as they become more complex. A formula that generalizes the results in Section 4 is still open, and its complexity is expected to increase with the size of the lattice graphs. We also hope to generate gluing formulae for other types of graphs, e.g. honeycomb graphs, and planar graphs in general.

We have discovered explicit formulae for the quadratic forms of the odd Laplacian and the incidence Dirac operator. Future work could be carried out to determine explicit formulae for the quadratic forms of the even and odd Dirac operators.

The case of Clifford graph algebras for disjoint gluings and bridge gluings of path graphs help to understand the space of spinors in higher dimensions. Further research in generalizing bridge gluings will be foundational in understanding the Clifford algebras of more complex graphs.

While our results on gluing formulae focus on the Clifford graph algebras defined by Khovanova [7], the Clifford algebras that represent spaces of spinors extend beyond those introduced. For example, $Cl(1, 3)^+$, the even part of the Clifford algebra $Cl(1, 3)$ is suitable for describing Dirac

spinors.[11] $Cl(1, 3)$ has four generators: one of which squares to $+1$, while the remaining three square to -1 . In order to allow for such a distinction under Khovanov's framework of Clifford graph algebras, we propose an additional graph coloring. We propose a form of Clifford graph algebra where vertices i are given a color based on their associated generator e_i , for example, red, if $e_i^2 = +1$, or blue, if $e_i^2 = -1$. Because the generators of Clifford algebras anticommute, their colored graphs are complete.

APPENDIX: ALGEBRAIC COMPUTATIONS FOR THE GLUING OF LATTICE GRAPHS

Corollary A.1. *The number of perfect matchings of $L_{3,n+m}$ is given by*

$$\begin{aligned} T_3(m+n) &= T_3(m)T_3(n) + T_3(m-1)T_3(n-1) \\ &\quad + \frac{(T_3(m+1) - T_3(m-1))(T_3(n+1) - T_3(m-1))}{2} \\ &\quad + \frac{(T_3(m) - T_3(m-2))(T_3(n) - T_3(n-2))}{2}. \end{aligned}$$

Proof.

$$\begin{aligned} T_3(m+n) &= \sum_B T_3(m \sqcup_{0,B} n) \\ &= T_3(m)T_3(n) + 2 \frac{(T_3(m+1) - T_3(m-1))(T_3(n+1) - T_3(m-1))}{4} \\ &\quad + 2(0) + 2 \frac{(T_3(m) - T_3(m-2))(T_3(n) - T_3(n-2))}{4} \\ &\quad + T_3(m-1)T_3(n-1). \end{aligned}$$

■

Proposition A.2. *The number of ways to tile $L_{3,n}$ with dominoes is given by the explicit formula*

$$\frac{(1 - (-1)^{n+1})(\alpha^{n+1} + (\frac{1}{\alpha})^{n+1})}{2\sqrt{6}},$$

where $\alpha = \frac{\sqrt{2} + \sqrt{6}}{2}$.

Proof. We can represent the recursion equation using matrices:

$$\begin{bmatrix} T_3(n+3) \\ T_3(n+2) \\ T_3(n+1) \\ T_3(n) \end{bmatrix} = \begin{bmatrix} 0 & 4 & 0 & -1 \\ 1 & 0 & 0 & 0 \\ 0 & 1 & 0 & 0 \\ 0 & 0 & 1 & 0 \end{bmatrix}^n \begin{bmatrix} T_3(3) \\ T_3(2) \\ T_3(1) \\ T_3(0) \end{bmatrix}.$$

By diagonalizing the recursion matrix and performing matrix multiplication, we find that

$$T_3(n) = \frac{3 - \sqrt{3}}{12} \left(\frac{-\sqrt{2} + \sqrt{6}}{2}\right)^n + \frac{3 - \sqrt{3}}{12} \left(\frac{\sqrt{2} - \sqrt{6}}{2}\right)^n + \frac{3 + \sqrt{3}}{12} \left(\frac{\sqrt{2} + \sqrt{6}}{2}\right)^n + \frac{3 + \sqrt{3}}{12} \left(\frac{-\sqrt{2} - \sqrt{6}}{2}\right)^n.$$

By rearranging, the formula becomes:

$$T_3(n) = \frac{\alpha^{n+1} - (\frac{-1}{\alpha})^{n+1}}{2\sqrt{6}} + \frac{(\frac{1}{\alpha})^{n+1} - (-\alpha)^{n+1}}{2\sqrt{6}} = (1 - (-1)^{n+1}) \frac{\alpha^{n+1} + (\frac{1}{\alpha})^{n+1}}{2\sqrt{6}}$$

where $\alpha = \frac{\sqrt{2} + \sqrt{6}}{2}$.

■

Proposition A.3. *The following identity holds:*

$$\sum_{i=0}^{n-2} T_4(i) = \frac{T_4(n) - T_4(n-3)}{5}.$$

Proof. $T_4(n) = T_4(n-1) + T_4(n-2) + 2 \sum_{i=0}^{n-2} T_4(i) + T_4(n-2) + T_4(n-4) + T_4(n-6) + \dots + (T_4(1) \text{ if } n \text{ is odd}) \text{ or } (T_4(0) \text{ if } n \text{ is even})$. By substituting $n-1$ for n , we see that $T_4(n-1) = T_4(n-2) + T_4(n-3) + 2 \sum_{i=0}^{n-3} T_4(i) + T_4(n-3) + T_4(n-5) + T_4(n-7) + \dots + (T_4(0) \text{ if } n \text{ is odd}) \text{ or } (T_4(1) + T_4(-1) \text{ if } n \text{ is even})$. Since $T_4(-1) = 0$, we can ignore that term. By adding these two equations together, we find that

$$\begin{aligned} T_4(n) + T_4(n-1) &= (T_4(n-1) + T_4(n-2) + 2 \sum_{i=0}^{n-2} T_4(i) \\ &\quad + T_4(n-2) + T_4(n-4) + T_4(n-6) + \dots \\ &\quad + (T_4(1) \text{ if } n \text{ is odd}) \text{ or } (T_4(0) \text{ if } n \text{ is even})) \\ &\quad + (T_4(n-2) + T_4(n-3) + 2 \sum_{i=0}^{n-3} T_4(i) \\ &\quad + T_4(n-3) + T_4(n-5) + T_4(n-7) + \dots \\ &\quad + (T_4(0) \text{ if } n \text{ is odd}) \text{ or } (T_4(1) + T_4(-1) \text{ if } n \text{ is even})) \\ &= T_4(n-1) + T_4(n-3) + 5 \sum_{i=0}^{n-2} T_4(i). \end{aligned}$$

From this equality, we can deduce that

$$\sum_{i=0}^{n-2} T_4(i) = \frac{T_4(n) - T_4(n-3)}{5}.$$

■

Proposition A.4. *The following identity holds:*

$$\sum_{i=1}^{\lfloor \frac{n}{2} \rfloor} T_4(n-2i) = -\frac{2}{5}T_4(n) + 4T_4(n-2) + \frac{7}{5}T_4(n-3) - T_4(n-4).$$

Proof. Again, we start with $T_4(n) = T_4(n-1) + T_4(n-2) + 2 \sum_{i=0}^{n-2} T_4(i) + \sum_{i=1}^{\lfloor \frac{n}{2} \rfloor} T_4(n-2i)$. From the previous proposition, we can rewrite this formula as $T_4(n) = T_4(n-1) + T_4(n-2) + 2 \frac{T_4(n) - T_4(n-3)}{5} + \sum_{i=1}^{\lfloor \frac{n}{2} \rfloor} T_4(n-2i)$. We also know that $T_4(n) = T_4(n-1) + 5T_4(n-2) + T_4(n-3) - T_4(n-4)$. The result follows from equating these two versions of $T_4(n)$ and solving for $\sum_{i=1}^{\lfloor \frac{n}{2} \rfloor} T_4(n-2i)$. ■

Corollary A.5. *The number of perfect matchings of $L_{4,n+m}$ is given by*

$$\begin{aligned} T_4(m+n) &= T_4(m)T_4(n) + T_4(m-1)T_4(n-1) \\ &\quad + \frac{2(T_4(m+1) - T_4(m-2))(T_4(n+1) - T_4(n-2))}{25} \\ &\quad + f(m+1)f(n+1) \\ &\quad + f(m)f(n). \end{aligned}$$

Where $f(n) = -\frac{2}{5}T_4(n) + 4T_4(n-2) + \frac{7}{5}T_4(n-3) - T_4(n-4)$.

Proof.

$$\begin{aligned}
T_4(m+n) &= \sum_B T_4(m \sqcup_{0,B} n) \\
&= T_4(m)T_4(n) + 4(0) + 2 \frac{(T_4(m+1) - T_4(m-2))(T_4(n+1) - T_4(n-2))}{25} \\
&\quad + f(m+1)f(n+1) \\
&\quad + f(m)f(n) \\
&\quad + 4(0) + T_4(m-1)T_4(n-1).
\end{aligned}$$

■

Proposition A.6. *The number of ways to tile $L_{4,n}$ with dominoes is given by the explicit formula*

$$\begin{aligned}
&\frac{\frac{6}{b} + 5 - \frac{1}{b^3}}{(1 - \frac{1}{b^2})(1 - \frac{b}{a})(1 - ab)} b^n - \frac{6b + 5 - b^3}{(1 - \frac{1}{b^2})(1 - \frac{b}{a})(1 - ab)} (\frac{1}{b})^n \\
&+ \frac{\frac{6}{a} + 5 - \frac{1}{a^3}}{(1 - \frac{1}{a^2})(1 - \frac{a}{b})(1 - ab)} a^n - \frac{6a + 5 - a^3}{(1 - \frac{1}{a^2})(1 - \frac{a}{b})(1 - ab)} (\frac{1}{a})^n,
\end{aligned}$$

where $a = \frac{1+\sqrt{29}+\sqrt{14+2\sqrt{29}}}{4}$ and $b = \frac{1-\sqrt{29}-\sqrt{14-2\sqrt{29}}}{4}$.

Proof. Use the same method as for the proof of Proposition A.2. ■

We conjecture that for every positive integer k , there exists a real number $x \in \mathbb{R}$ such that the solutions to the equation $\frac{x^5+1}{x^2(x+1)} = \frac{y^5+1}{y^2(y+1)}$, which are at most two pairs of reciprocal numbers, denoted $y_1, \frac{1}{y_1}, y_2, \frac{1}{y_2}$ allow us to define functions $f_{k,1}(y_1, y_2), f_{k,2}(y_1, y_2), f_{k,3}(y_1, y_2), f_{k,4}(y_1, y_2)$ such that $T_k(n) = f_{k,1}(y_1, y_2)y_1^n + f_{k,2}(y_1, y_2)\frac{1}{y_1}^n + f_{k,3}(y_1, y_2)y_2^n + f_{k,4}(y_1, y_2)\frac{1}{y_2}^n$, where $T_k(n)$ is an explicit formula for the number of ways to tile $L_{k,n}$.

REFERENCES

- [1] David Cimasoni and Nicolai Reshetikhin, *Dimers on surface graphs and spin structures. i*, Communications in Mathematical Physics **275** (2007), no. 1, 187–208.
- [2] Ivan Contreras, Michael Toriyama, and Chengzheng Yu, *Gluing of graph laplacians and their spectra*, Linear and Multilinear Algebra **68** (2020), no. 4, 710–749.
- [3] Ivan Contreras and Boyan Xu, *The graph laplacian and morse inequalities*, Pacific Journal of Mathematics **300** (2019), no. 2, 331–345.
- [4] Pieter Kasteleyn, *Graph theory and crystal physics*, Graph theory and theoretical physics, (1967), pp. 43–110.
- [5] Richard Kenyon, *The laplacian and dirac operators on critical planar graphs*, Inventiones mathematicae **150** (2002), no. 2, 409–439.
- [6] ———, *An introduction to the dimer model*, arXiv (2003), math/0310326.
- [7] Tanya Khovanova, *Clifford algebras and graphs*, arXiv (2008), math/0810.3322.
- [8] Oliver Knill, *The Dirac operator of a graph*, arXiv (2013), math/1306.2166.
- [9] Pavel Mnev, *Graph quantum mechanics*, Contribution to the 2016 MPIM Jahrbuch (2016).
- [10] Bogdan Nica, *A brief introduction to spectral graph theory*, European Mathematical Society, Zürich, (2018).
- [11] Pierre Renaud, *Clifford Algebras Lecture Notes on Applications in Physics*, (2020).
- [12] Nicolai Reshetikhin and Boris Vertman, *Combinatorial Quantum Field Theory and Gluing Formula for Determinants*, Lett. Math. Phys. **105** (2015), no. 3, 309–340.
- [13] Chengzheng Yu, *Super-walk formulae for even and odd laplacians in finite graphs*, Rose-Hulman Undergraduate Mathematics Journal **18** (2017).

DEPARTMENT OF MATHEMATICS, YALE UNIVERSITY, YALE UNIVERSITY, 442 DUNHAM LAB, 10 HILLHOUSE AVE,
NEW HAVEN, CT 06511

Email address: `beata.casiday@yale.edu`

DEPARTMENT OF MATHEMATICS AND STATISTICS, AMHERST COLLEGE, 31 QUADRANGLE DRIVE, AMHERST, MA
01002

Email address: `icontreraspalacios@amherst.edu`

Email address: `tmeyer23@amherst.edu`

Email address: `espingarn23@amherst.edu`

DEPARTMENT OF MATHEMATICS, UNIVERSITY OF CHICAGO, ECKHART HALL, 5734 S UNIVERSITY AVE, CHICAGO
IL, 60637

Email address: `scmi@uchicago.edu`